MICROCOPY RESOLUTION TEST CHART

NATIONAL BUREAU OF STANDARDS 1963 A

DTIC

①

INVESTIGATION OF
PSEUDO BI-POLAR NICKEL CADMIUM BATTERIES
AS
FILTER ELEMENTS FOR PULSED POWER LOADS

THESIS

Michael B. Cimino   Gregory M. Gearing
   Major, USAF   Captain, USAF

AFIT/GE/ENG/84D-18

DTIC
ELECTE
APR 1 1985
S D
B

DEPARTMENT OF THE AIR FORCE

AIR UNIVERSITY

AIR FORCE INSTITUTE OF TECHNOLOGY

Wright-Patterson Air Force Base, Ohio

85   03   13   061

INVESTIGATION OF
PSEUDO BI-POLAR NICKEL CADMIUM BATTERIES
AS
FILTER ELEMENTS FOR PULSED POWER LOADS

THESIS

Michael B. Cimino   Gregory M. Gearing
    Major, USAF   Captain, USAF

AFIT/GE/ENG/84D-18

DTIC
ELECTE
APR 1 1985
S
B

INVESTIGATION OF

PSEUDO BIPOLAR NICKEL CADMIUM BATTERIES

AS

FILTER ELEMENTS FOR PULSED POWER LOADS

THESIS

Presented to the Faculty of the School of Engineering

of the Air Force Institute of Technology

Air University

In Partial Fulfillment of the

Requirements for the Degree of

Master of Science in Electrical Engineering

Michael B. Cimino   Gregory M. Gearing

Major, USAF   Captain, USAF

December 1984

Preface

The authors wish to express their appreciation to all who have sacrificed their time and energies on our behalf. Particularly valuable were the contributions of Mr. W. Scott Bishop, Dr. David Fritts, and Mr. John Leonard of the Air Force Wright Aeronautical Laboratories, Aero Propulsion Laboratory, Mr. Ron Ruley of the Model Fabrication Division of the Air Force Institute of Technology, and also our fathers, Mr. S. Michael Cimino and Mr. Albert Gearing.

Mike Cimino
Greg Gearing

ii

Table of Contents

iii

List of Figures

vi

List of Tables

Abstract

This investigation consisted of several tests of specially fabricated nickel-cadmium batteries having circular disk type electrodes. These batteries were evaluated as filter elements between a constant current power supply and a five hertz pulsed load demanding approximately twice the power supply current during the load on portion of the cycle. Short tests lasting 10^4 cycles were conducted at up to a 21 C rate and an equivalent energy density of over 40 Joules per pound. In addition, two batteries were subjected to 10^7 charge/discharge cycles, one at a 6.5 C rate and the other at a 13 C rate. Assuming an electrode to battery weight ratio of 0.5, these tests represent an energy density of about 7 and 14 Joules per pound respectively. Energy density, efficiency, capacitance, average voltage, and available capacity were tracked during these tests. After 10^7 cycles, capacity degradation was a negligible for one battery and about 20% for the other. Cadmium electrode failure may be the factor limiting lifetime at extremely low depth of discharge cycling. The output was examined and a simple equivalent circuit was proposed.

I - Introduction

Background

Satellite power systems have grown steadily since Sputnik first orbited the earth with a modest battery powered electrical system. Even though this system functioned for only three weeks, it accounted for 38% of the satellite's weight [16]. N.J. Stevens of the Space Communications Group, Hughes Aircraft Company, recently pointed out that "There have been several proposals for future space missions that will require power generation capabilities in excess of 100 KW's" [15]. In order to meet these expanding requirements larger and larger power conditioning systems will have to be built.

Unless a significant increase in the energy density (joules per pound) of power sources can be obtained, this trend means a continual increase in power supply weight. In 1982, A.S. Gilmour of the State University of New York reported that [10]:

> The launch to low earth orbit (LEO) of systems as large or larger than 50 kW is now possible with the space shuttle. The transfer of these high power systems to higher orbits is not presently possible because of weight limitations. To make transfer to higher orbits possible, system weight must be reduced.

Capacitive filters are currently used to provide high load current pulses to reduce the peak current demanded of the power source. In addition, capacitors rapidly store

1

energy supplied from the source during the load off portion of the duty cycle. This reduction in required delivery of high peak current reduces the size of a given power source which is dependent upon peak current and voltage. However, the weight of the filter capacitors cannot be neglected.

According to W.S. Bishop of the Air Force Wright Aeronautical Laboratories, Wright Patterson AFB, "Capacitors are expected to deliver about 1 joule per pound for these applications" [4]. An initial test conducted by W.S. Bishop and D.C. Stumpff demonstrated the possibility of a 10-fold increase in energy density by replacing the capacitive filter with nickel-cadmium batteries. In their report, they point out that "this (increase in) energy density would result in a weight savings of up to 4500 pounds for one conceptual high power satellite electrical system" [5]. The nickel-cadmium batteries would deliver more than 10 joules per pound - a significant improvement over present capabilities.

However, their test did not optimize battery usage; rather it only served to demonstrate that batteries appear to be a competitive alternate to capacitors. Although their test demonstrated 10^7 cycles of operation at 5 hertz, one proposal, for a 10 year life span, would require over 10^9 cycles, more than 100 times the value achieved.

There are many unknowns factors in battery operation which need to be understood, so that batteries may be opti-

2

mized, before the well known and reliable capacitors now in use can be replaced by them. For example, battery shelf life, cycle life, temperature dependence, and the relationship of physical geometry and chemical properties to electrical performance are all areas yet to be adequately investigated with the intent to make batteries capable of out performing capacitors as power supply filters.

Purpose

This thesis investigated the use of nickel-cadmium batteries as filter elements between a continuous DC power source and a pulsed load. The objective was to verify a possible electrode characteristic that could optimize a battery for this task, to accurately assess the battery's electrical operation during cycling, and to estimate expected battery life by conducting a 10^7 cycle life test.

Scope

This investigation consisted of several tests of fabricated nickel-cadmium cells having circular disk type electrodes. These tests addressed three areas.

1. Will the use of circular electrodes increase the available energy density when compared to the standard aircraft batteries, as tested by Bishop and Stumpff [5] ?

2. What energy density could be achieved if a cycle lifetime of 10^9 pulses at 5 hertz is specified?

3.   How does the battery influence voltage and current
     waveforms to the load?

Approach

The procedure started with the construction of several
four cell pseudo bi-polar nickel-cadmium batteries using
circular electrodes. The first step was to find a way to
minimize the electrolyte leakage through the nickel-plexi-
glas joint in the intercell separator. Next, to insure
uniformity between cells and batteries during testing, all
electrodes were sintered and electrochemically loaded with
nickel oxide either by Eagle Picher Industries, Colorado
Springs, Colorado, or by using the D.F. Pickett process at
the Air Force Wright Aeronautical Laboratories/Aero Propul-
sion Laboratory (AFWAL/APL), Wright Patterson AFB, Ohio
[14]; or loaded with cadmium using the Fritts, et. al.
impregnation technique at AFWAL/APL [8]. The weight of each
cell's electrodes was measured for later evaluation of the
energy density.

Next, the cells were assembled and filled with electro-
lyte solution, completing the battery construction. Cadmium
wire probes (reference electrodes) were also inserted in
each cell to monitor battery performance.

The initial tests paralleled those of Bishop and
Stumpff. Energy densities achieved in this test (circular
electrodes) were compared to Bishop and Stumpff's results

4

(rectangular electrodes), providing a comparison of electrode types. The second series of evaluations attempted to establish a relationship between expected service life (in number of charge/discharge cycles) versus depth of discharge relationship, using a shortened life cycle test.

The third area of interest was to evaluate the battery influence on the voltage and current supplied to a pulsed load. This was accomplished both during and after the 10^7 cycle test.

Sequence of Presentation

Chapter 2 discusses the theory of a battery's operation and the characteristics that make it useful as a filter. Chapter 3 explains bi-polar battery theory and the construction of the test batteries. Chapter 4 describes the experimental procedures used. Chapters 5 and 6 discuss the results and conclusions of the testing. Appendices A and B contain detailed battery drawings, discussion of construction problems, and description of the electrode loading process. Appendices C and D contain a list of test equipment, calibration data, and test data.

II - Battery Theory

Background

Many types of batteries and fuel cells are available today, some of which have shown the possibility of better lifetime, energy density, or temperature operating limits than the nickel-cadmium battery. This paper has focused on the nickel-cadmium battery because of its widespread use, particularly in space applications, and its overall performance capability. Table 2-1 shows a comparison of various types of rechargeable batteries currently available for use.

TABLE 2-1 [3]
AIRCRAFT BATTERY OPTIONS

BATTERY TYPE → CHARACTERISTICS ↓	NICKEL CADMIUM	LEAD ACID	NICKEL ZINC	SILVER ZINC
WEIGHT	Heavy	Heaviest	Light	Lightest
VOLUME	Large	Large	Small	Smallest
COST	Moderate	Lowest	Moderate to low	Highest
POWER DENSITY	High	Lowest	High	Highest
CALENDAR LIFE	Good	Good	Good	Poor
CYCLE LIFE	Good	Fair	Fair	Poor
LOW TEMP. OPERATION	Best	Fair	Fair	Poorest

6

Nickel-Cadmium Batteries

Additionally, extensive testing of nickel-cadmium batteries has been conducted both by and for NASA (i.e. Life Cycle Testing conducted by the Naval Weapons Support Center (NWSC CRANE) in Crane, Indiana for the past 20 years). These tests have, however, centered on classical storage battery applications characterized by relatively long (1/2 - 2 hour) discharge and (1 - 23 hour) charge cycles at deep depths of discharge (DOD). Under these circumstances the dominating processes are the electrochemical reactions at the electrodes as opposed to the double layer capacitance effect which will be discussed later.

Chemical Reactions

Figure 2-1 shows a simple single cell nickel-cadmium battery. The three elements are the nickel oxi-hydroxide (NiO(OH)) coated positive electrode, the cadmium (Cd) coated negative electrode, and the aqueous potassium hydroxide (KOH) electrolyte.
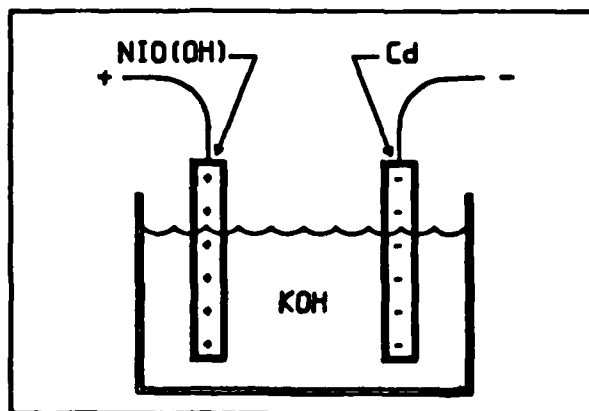
SIMPLE NICKEL CADMIUM BATTERY
FIGURE 2-1

7

The chemical reaction at the positive electrode is between the active material, NiO(OH), and the KOH electrolyte. At the negative electrode, the reaction is between the active material, Cd, and the the electrolyte.

During discharge, the NiO(OH) at the positive electrode accepts electrons from the external circuit, decaying to the lower state of $Ni(OH)_2$ and releasing an OH^- ion. The electrolyte passes this ion to the negative electrode, where it combines with the cadmium forming cadmium hydroxide $Cd(OH)_2$ and emitting two electrons to the external circuit. Milner and Thomas [12] express the chemical reaction during discharge as:

$$2[e^- + 2H_2O + NiO(OH) \rightarrow Ni(OH)_2 \cdot H_2O + OH^-] \tag{1}$$

and,

$$Cd + 2OH^- \rightarrow Cd(OH)_2 + 2e^- \tag{2}$$
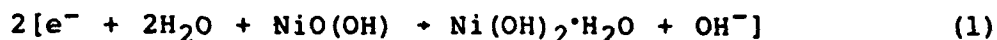
During the recharge of the battery the reverse is true. The individual electrode reactions can be combined into one equation:

$$Cd + 2H_2O + 2NiO(OH) \overset{\text{Charge} \rightarrow}{\underset{\leftarrow \text{ Discharge}}{=}} 2Ni(OH)_2 + Cd(OH)_2 \tag{3}$$
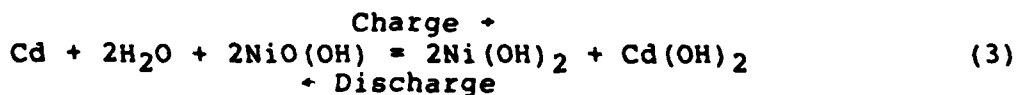
to describe the net overall chemical reaction occurring in the battery.

Double Layer Capacitance Effect

The previous equations (1-3) describe the classical electrochemical process occurring in the battery during both charging and discharging. However, these are only the longer term (seconds and greater) effects of the battery operation. When used for filtering the voltage to a pulsed load, an instantaneous current change with a zero change in voltage is desired. The leading edge of the current pulse, and voltage output from the nickel-cadmium battery is shaped by its short term or transient characteristics. These characteristics are dominated by the battery's double layer capacitance and internal resistance.

A typical capacitor is composed of two metal, or conducting plates separated by a dielectric material. The equation:

$$\text{charge (Q)} = \text{capacitance (C)} \times \text{voltage (V)} \qquad (4)$$

describes its operation. As current flows into a capacitor, charging it, a voltage can be measured between the two plates. Chemically, concentration of positive charges (depletion of ions) will form on one plate, while on the other plate a concentration of negative charges (ions) will form. These two charged areas are separated by the thickness of the dielectric material.

In much the same way, when a nickel-cadmium battery is charged, the electrolyte forms several layers of charged

9

ions near each electrode. Each layer of charged ions is separated by water molecules which act as the dielectric medium between the layers. The cell voltage, across each electrode-electrolyte junction, spans these charged ion layers. These layers are known as the electrical double layers, since the ion interaction takes place predominately in the two layers closest to the electrode.

This "double layer" charge and voltage characteristic, called double layer capacitance, is an important factor in the initial rate of change of both the voltage and current when the battery is switched between charging and discharging operations. It is particularly significant for battery applications at the higher cyclic rate of 5 Hertz. A common nickel-cadmium battery equivalent circuit is shown in Figure 2-2. E is an ideal voltage source, R1 is the effective delayed internal resistance, R2 is the effective instantaneous internal resistance, and C is the effective double layer capacitance of the electrodes.

Although the exact cause and values of these capacitances are not precisely known, a typical range is from 50 to 2200μF/cm^2. Amile, et. al. [1] reported that the double layer capacitance of the nickel electrode was approximately 2100μF/cm^2 and that of the cadmium electrode was approximately 50μF/cm^2.
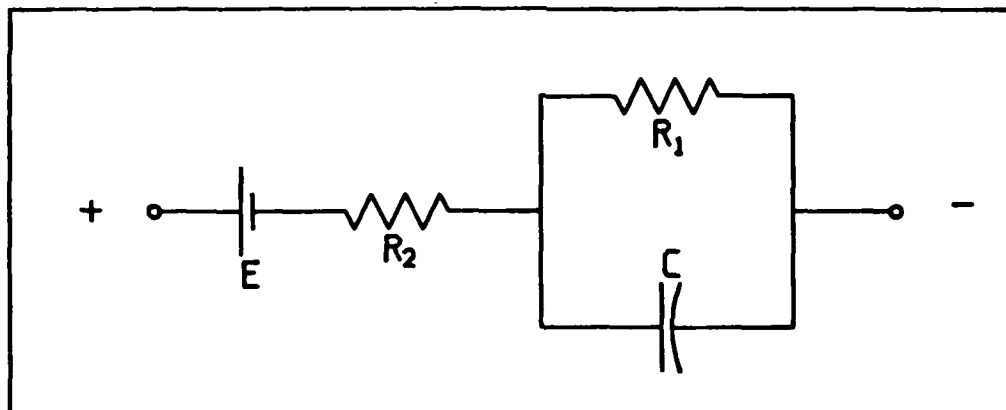
NICKEL CADMIUM BATTERY EQUIVALENT CIRCUIT
FIGURE 2-2

The current through a capacitor is proportional to both the capacitance and rate of change of voltage by:

$$i = C(dv/dt) \tag{5}$$

This indicates that a larger capacitor will have a lower rate of voltage drop for a given current flow. Similarly a larger double layer capacitance in a battery should provide an increase in available current during the initial rise in current to a pulsed load while also limiting the voltage drop.

The double layer capacitances and faradaic discharge all have different time responses. The double layer capacitances with the delayed internal resistance form an effective decay time constant in milliseconds. The faradaic decay is over minutes to hours. It is reasonable therefore, to consider the nickel-cadmium battery's response to a

11

pulsed load in three phases, although all three occur simul-
taneously.

First, when the load is applied, the initial drop in
voltage will be from the negative electrode (cadmium) double
layer capacitance discharging. Next the positive electrode
(nickel) double layer capacitance will discharge. These
first two steps comprise the short term or transient charac-
teristic of the battery. The final step is the classical
electrochemical, or faradaic, discharge through the
electrolyte.

If the double layer capacitance, internal battery re-
sistance, and the classical slope of the voltage decrease/
increase versus capacity can be determined, then it may be
possible to derive an equivalent circuit to predict the
effect a battery will have when inserted as a filter element
into a circuit.

The effective double layer capacitance of the battery
can be calculated as follows, assuming that the capacitance
of the battery remains constant. Pick a value of i and the
corresponding dv/dt from the voltage and current waveforms
of the battery input/output. By rearranging equation (5)

$$C = i/(dv/dt). \qquad (6)$$

12

Example:

$$i = 13 \text{ amperes}$$

$$dv/dt = 9 \text{ volts/second}$$

from equation (6)

$$C = [13 \text{ amperes}/9 \text{ volts/second}]$$

$$= 1.4 \text{ farads}$$

There are two ways of determining the internal resistance. One is to measure the impedance with an a-c ohmmeter. The other is to assume that the instantaneous voltage change when the battery is switched from charging to discharging is strictly an IR drop. The resistance then, is simply the change in voltage divided by the change in current (dv/di). The voltage versus capacity can be plotted by recording the battery voltage while charging and discharging the battery with a constant current.

Battery Testing

Most, if not all, nickel-cadmium battery use has involved deep discharge followed by a slow recharge. Some commercial applications, such as electric shavers, calculators, and flashlights, discharge the battery to a depth of 50 to 80 percent of capacity in 1 to 3 hours and then recharge in 10 to 12 hours, or "overnight" [9]. Currently, satellite operations use batteries to supply power during the "dark period" of an orbit. Typically a 1/2 to 2 hour discharge followed by a 1 to 23 hour recharge [13].

As a result, most testing of batteries has focused on DOD's from 15 to 80 percent [13] and recharge rates from 0.1 to 1 C (C is defined as the rated value of current that will discharge a battery in one hour). Results of tests at these deep DOD's have yielded lifetimes of 500 to 30,000 cycles for commercial applications [9], and NASA/USAF lifetimes of 1000 to 50,000 cycles [13] before the battery capacity decreases to 50% of its initial rated capacity.

The data of actual long term testing of many different types of batteries at NWSC CRANE [13] indicates that cycle lifetime is inversely related to DOD. That is, at a lower DOD, a battery will last longer (more cycles) than it does at a higher DOD. The use of batteries as filter elements in spacecraft power systems may need 10^9 cycles or more of operation, if run at a 5 hertz rate for a 10 year period. To achieve this cycle lifetime, a reduced DOD, possibly as low as one-tenth of one percent, may be required.

Energy Density

The energy density of a battery is directly related to its operational DOD. For example, if a 1.2 volt, 22 ampere/ hour battery is operated at a DOD of 0.01% and a 5 hertz rate, it delivers approximately 10 joules of energy per cycle. If the battery weighs 10 pounds, then its energy density would be 1 Joule per pound. However, if the DOD could be increased to 0.1%, the same battery, would be

14

delivering 100 Joules of energy, with a new energy density of 10 Joules per pound!

Bishop and Stumpff [5] found that approximately a 60% capacity degradation occurred in a 10^7 cycle test at 0.013% DOD. This DOD equated to an energy density of approximately five Joules per pound. They also demonstrated an energy density of 11.4 Joules per pound, although only for a short time due to conductor and battery heating.

During their test, battery usage was not optimized, nor were elaborate precautions taken to eliminate test equipment induced inductance and capacitance. The test served only to demonstrate the feasability of nickel-cadmium batteries replacing capacitors as low frequency filter elements.

Since energy density and DOD are directly related, an increase in DOD corresponds to a increase in energy density. Such an increase is, however, achieved at a cost of reduced lifetime, since many failure mechanisms are also accelerated by increases in DOD. Heating, mechanical stress, electrode material migration, and separator failure are all examples of common nickel-cadmium battery failure mechanisms.

Heating, in the form of I^2R losses due to internal resistances, may be influenced directly by choices of material and battery geometry. Heating of the electrode battery posts was identified as a major problem area during the tests by Bishop and Stumpff.

15

Dr. D.H. Fritts of the Air Force Wright Aeronautical Laboratories has hypothesized that one of the limiting aspects of Bishop and Stumpff's test was the uneven current flow through the electrodes of the standard aircraft batteries used during their test [7]. Further, he has suggested that the use of circular electrodes might reduce this problem by increasing the maximum available current flow, and thereby increasing the energy density achievable.

Assuming that internal heat generation is a primary cause of battery failure, reducing this stress should allow an increased operating life [5,7,13]. Alternatively, if the internal resistance is reduced, the current could be increased, while still operating the battery at the same stress level. A higher current would mean a higher DOD and therefore a higher energy density.

The battery described in this paper has attempted to reduce the internal resistance and thereby the I^2R loss, by using circular electrodes and increasing the cross sectional area, while reducing the length, of the internal conductor. In short, using a pseudo bi-polar battery. This battery design is described in Chapter 3 and Appendices A and B.

16

III - Experimental Battery

Background

In order for batteries to successfully replace capacitive filter elements in large space electrical power systems, they must posses two characteristics. First, the battery system must be significantly lighter than the conventional system and still be capable of providing the desired power conditioning. Secondly, the system must survive for the duration of the assigned mission, 10 years in one proposed scenario.

These two qualities are often diametrically opposed in a battery. Steps to improve one may jeopardize the other. For example, if the DOD is increased to reduce the required battery weight, the cycle life of the battery will be reduced. This relationship can be seen in the classical log-cycle-life versus DOD plot, reproduced in Figure 3-1 from a NASA study of batteries for space applications [2].

Extrapolation to low DOD's appears to limit the cycle life to less than 10^5 cycles. However, the study by Bishop and Stumpff demonstrated 10^7 cycles of operation at a DOD of 0.013%. This is not an unreasonable result, since the classical plot is a straight line approximation based on data taken at moderate to high DOD's. For example, extensive life cycle testing of batteries at NWSC CRANE has been conducted for more than 20 years [13]. These tests are

17

12 A-H NICKEL-CADMIUM CELLS

O	49 C (120 F)
□	24 C (75 F)
▷	-18 C (0 F)
●	-34 C (-30 F)

CYCLE LIFE, CYCLES

CYCLIC LIFE VERSUS DEPTH OF DISCHARGE
FIGURE 3-1 [2]
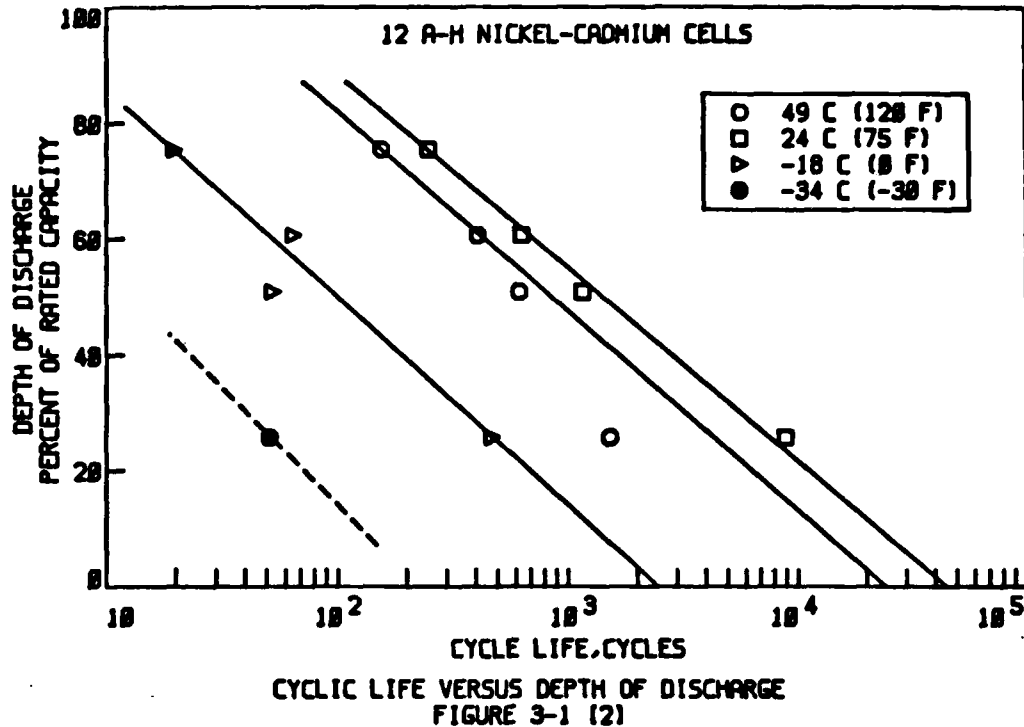
primarily at DOD's greater than 15% and are conducted on a real time basis, often lasting several years.

Accelerated life cycle testing is a questionable proposition at best. Some approaches, such as Goddard Space Flight Center's Accelerated Test Plan for Nickel Cadmium Batteries have been proposed [11]. This proposal would require extensive testing and diagnosis of many cells, far beyond the scope of this thesis. Further, Paul Bauer [2] asserts that accelerated testing is very dependent on prior understanding of a specific cell's failure mechanisms and their relationship to external factors. In the absence of

such detailed knowledge, one may accelerate a failure mode that would not be a factor during normal operations.

Actual life cycle test data at extremely low DOD's is almost non existent. Though the test by Bishop and Stumpff is by no means conclusive, it does indicate the possibility of long cycle life at extremely low DOD's and relatively high cycling frequencies (5 hertz).

Assuming that the proper design with a suitably picked DOD can achieve the desired cycle life, increasing the batteries energy density and thereby reducing the weight required to do a given task is the next step.

Bi-Polar Battery

Initially considered was the pile or bi-polar geometry. As pointed out by Bauer [2], the bi-polar battery's advantage is its extremely low internal resistance and inductance, enabling it to deliver pulses of high current for short periods. The reduced internal losses lead to greater efficiency and therefore the potential for a higher energy density.

The reduction is achieved by straightening and shortening the current path within the battery. Unlike the common mono-polar battery, in which individual cells are externally connected in series, the bi-polar battery consists of a stack of cells. All internal electrodes have both a positive and negative side, eliminating the need for

19
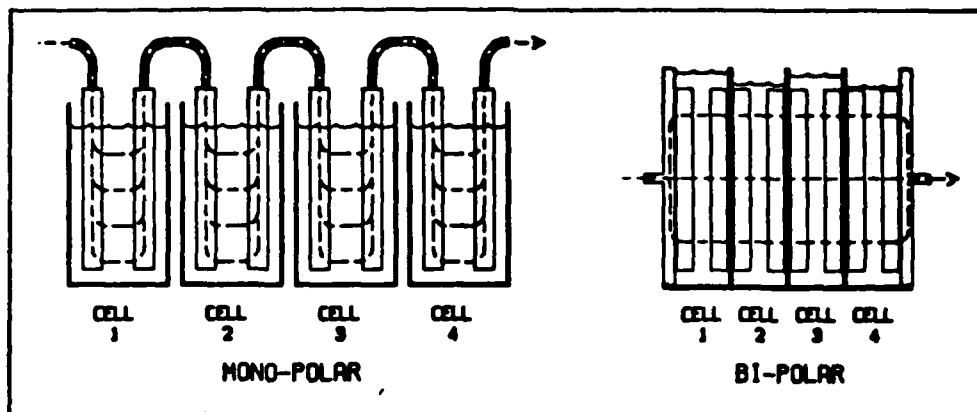
CURRENT PATH THROUGH A 4 CELL BATTERY
FIGURE 3-2

for current to flow out of one cell's electrode and then
through some interconnecting path, with inevitable losses,
simply to enter the next cell. Figure 3-2 illustrates these
differences.

Bi-polar electrodes have been formed on foil substrates
that have varied from 0.076 to 0.5 mm thick [6]. A sinter,
typically nickel, is formed on both sides and loaded with
active material, nickel hydroxide on one side and cadmium on
the other. Thus the foil substrate acts as the cell wall as
well as the intercell electrical connection. Although the
construction of bi-polar electrodes has been accomplished at
a number of facilities, the fabrication of a bi-polar bat-
tery has been complicated by the lack of a reliable edge
seal to prevent electrolyte shorting between cells.

Pseudo Bi-Polar Battery

In order to take advantage of the bi-polar geometry without inheriting the edge seal problems, a battery was designed specifically for use in this project, with a short current path. It resembles a monoblock type construction frequently used in automotive type batteries and consists of a stack of single cell button style batteries in which adjoining cells share a common wall and intercell connector. Figure 3-3 shows an exploded view of the battery design. Specific details and drawings are in Appendix A. To obtain some understanding of the effects of this design on internal losses and to be compatible with available test equipment, four cell nickel cadmium pseudo bi-polar batteries were constructed.

In order to further reduce internal losses, a circular electrode with a large central current tab to uniformly collect the current was selected. The electrode was a 3.3 inch diameter disc with the active material impregnated in an annular shape around the center 1.25 inch diameter current tab. Current flow within the electrode should be radial and the maximum current path length from the tab to the edge of the electrode is approximately 1.03 inches. This is in contrast to typical nickel cadmium aircraft batteries which have rectangular electrodes with a current tab in one corner.

21

PLEXIGLAS WALL

NEGATIVE TERMINAL
CADMIUM ELECTRODE

CELL 4

SEPARATOR

NICKEL ELECTRODE
INTER-CELL CONNECTOR

PLEXIGLAS WALL

CADMIUM ELECTRODE

SEPARATOR

CELL 3

NICKEL ELECTRODE
INTER-CELL CONNECTOR

PLEXIGLAS WALL

CADMIUM ELECTRODE

SEPARATOR

CELL 2

NICKEL ELECTRODE
INTER-CELL CONNECTOR

PLEXIGLAS WALL

CADMIUM ELECTRODE

SEPARATOR

CELL 1

NICKEL ELECTRODE
POSITIVE TERMINAL
PLEXIGLAS WALL

PLEXIGLAS CASE

EXPANDED VIEW OF THE TEST BATTERY
FIGURE 3-3
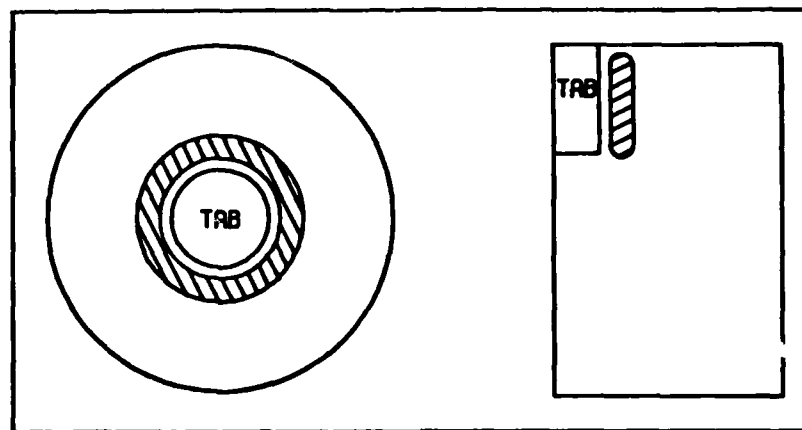
CIRCULAR VERSUS RECTANGULAR ELECTRODES
FIGURE 3-4

Figure 3-4 illustrates the differences between the test battery's electrode and that of a typical rectangular battery's electrode. The cross hatched areas are regions of highest current density. For rectangular electrodes, this area, between the positive and negative current tabs, has been identified as a stress point and is associated with sealed battery failures [7]. Although the circular tab does not eliminate this problem, it is a step towards a bi-polar design where the current density is spread more uniformly over a larger area of the electrode, thereby reducing the stress and attendant failure mechanisms.

The cells are electrically connected by a 1.125 inch diameter, 0.210 inch thick nickel slug mounted in the plexiglass wall. The large cross section and relatively short intercell path length result in both a smaller internal

resistance and inductance through the battery. The nickel
to plexiglas seal was established by using an O-ring around
the nickel slug.

The positive nickel electrodes were obtained from Eagle
Picher Industries. The plaque material was a standard 0.030
inch thick nickel sinter (dry sinter process) with a porosi-
ty of 80%. They were electrochemically impregnated with 1.7
grams of active NiO(OH) per cubic centimeter of void. The
result was an electrode with approximately a 1.4 ampere hour
theoretical capacity. In addition, to improve the elec-
trode/nickel slug weld, Battery 7 was constructed with nick-
el electrodes fabricated at AFWAL/APL using the D.F. Pickett
process [14], to approximately the same 1.4 ampere hour
theoretical capacity.

The negative cadmium electrodes supplied by Eagle
Picher Industries were difficult to weld satisfactorily to
the nickel slug intercell connector. Therefore the cadmium
electrodes were fabricated at AFWAL/APL using a process
developed and patented by Fritts, et. al. [8]. This process
used the same base plaque, 0.030 inch thick 80% porosity
nickel sinter. The electrodes were loaded with 6 to 8 grams
of active cadmium each for a theoretical capacity of 2.5 to
3.1 ampere hours. This combination insured that the battery
cells were nickel limited.

24

The cells were assembled by first welding the elec-
trodes to the nickel slug/plexiglas wall combination. Then
these units were stacked and glued one by one in a plexiglas
tube. A relief vent (about 8 psi) was installed in each
cell. Finally a reference electrode, a one millimeter dia-
meter cadmium wire was inserted into each cell. Leads were
soldered on the outside of the end cells and a plexiglas
stand was attached.

To fill the cells the vents were removed and the bat-
tery was set upside down in a beaker of electrolyte (32% by
weight KOH). A vacuum of 28 inches of mercury was pulled on
the entire assembly. When the vacuum was released, electro-
lyte was drawn into the cells. This procedure was repeated
several times to insure electrode saturation.

The weight of the beaker, KOH, and battery was taken
before and after filling the first two batteries to insure
that water removed during the vacuum filling would not
affect the KOH concentration. Evaluation revealed a loss of
only 1 gram of water per liter of KOH representing less than
0.1% change in KOH concentration. Subsequent batteries were
not weighed prior to filling. Specific details and adjust-
ments made during the battery fabrication are contained in
Appendices A and B.

IV - Experimental Test Procedure

Finding a Seal

One of the major problems with the construction and use of bi-polar batteries is obtaining a satisfactory intercell seal, thus keeping the electrolyte from shorting out adjoining cells. The first step in the fabrication of the test battery was to evaluate a neoprene O-ring placed around a nickel slug. This assembly was then inserted in the bottom of the test container as shown in Figure 4-1. The bottom of this container simulated an intercell wall. The test was initially run using a custom made O-ring with a glue joint. Although the seal held, the KOH reacted with the glue, weakening the joint and contaminating the electrolyte.

A standard sized, one piece O-ring was then tested. There was no noticeable electrolyte leakage in 30 days, with a 32% by weight KOH solution under approximately 8 psi of pressure. This success, elimination of electrolyte leakage between cells, overcame one of the major stumbling blocks in bi-polar nickel-cadmium battery construction.

Electrode Comparison

Prior to final construction, the electrodes for each battery were weighed. The weight of each assembled battery, including electrolyte, was recorded. Separate weights were taken, since the overall battery container was not optimized for weight, but rather for ease of construction in the
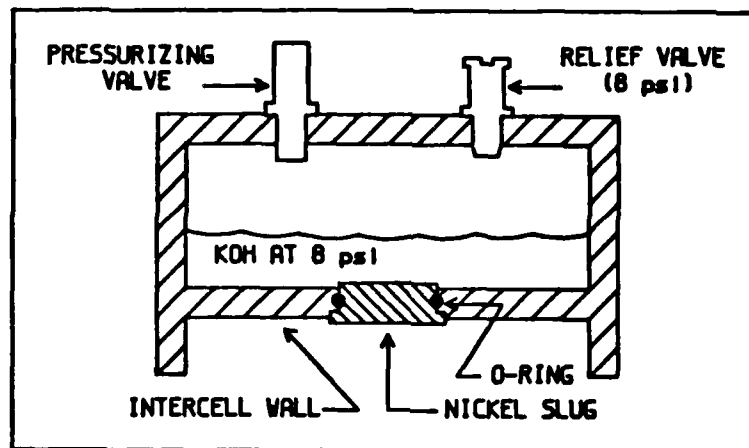
CUTAWAY OF O-RING SEAL TEST CONTAINER
FIGURE 4-1

laboratory. As a comparison, the electrode weight of the batteries used by Bishop and Stumpff [5] was 6.40 pounds while their total battery weighed 11.7 pounds. Therefore, the electrode accounted for 54.65% of the total weight. This ratio was used to determine the weight figure used in energy density calculations. It is based on the assumption that with some technological improvements, the test battery's design would result in a similar electrode to battery weight ratio.

Another important factor in battery design is the electrode surface current density. In normal parallel plate construction, each side of an electrode acts as a separate electrode, so that one half of the current flows from the center screen through each side of the electrode. However, rather than metal foil separating the cells, as in a true bi-polar battery, this pseudo bi-polar nickel-cadmium battery used a nickel slug and plexiglas intercell wall.

27

For Bishop and Stumpff, the current density through the electrode surface, with a total current of 100 amps, was 0.0458 amperes/cm^2. The test electrodes, although designed to be used in a double sided configuration, were used as single sided electrodes. As a result, the current density for the test batteries, based on a single sided current flow, with a charging/discharging current of 6.36 amperes, was 0.136 amperes/cm^2. This results in possibly greater polarization at the electrode/electrolyte interface of the test batteries.

Test Set Up

Figure 4-2 shows the equipment and circuit used for these tests. Two separate circuits were set up. The first had a 0-15 ampere load and the second had a 0-60 ampere load. A 0-50 amp, constant current, constant voltage power supply, was connected in parallel, and on opposite sides of the battery, with either a 0-15 ampere solid state load, or a 0-60 ampere solid state load. A 5 hertz square wave generator switched the load, simulating a 50% duty cycle current pulse load. A blocking diode on the output of each power supply prevented an inadvertent battery discharge back through the power supply. Current shunts were inserted as shown in Figure 4-2 to measure actual power supply current (I_S), load current (1_L), and battery current (I_B). Note that for battery charging, I_B is negative and for discharging I_B is positive.

28
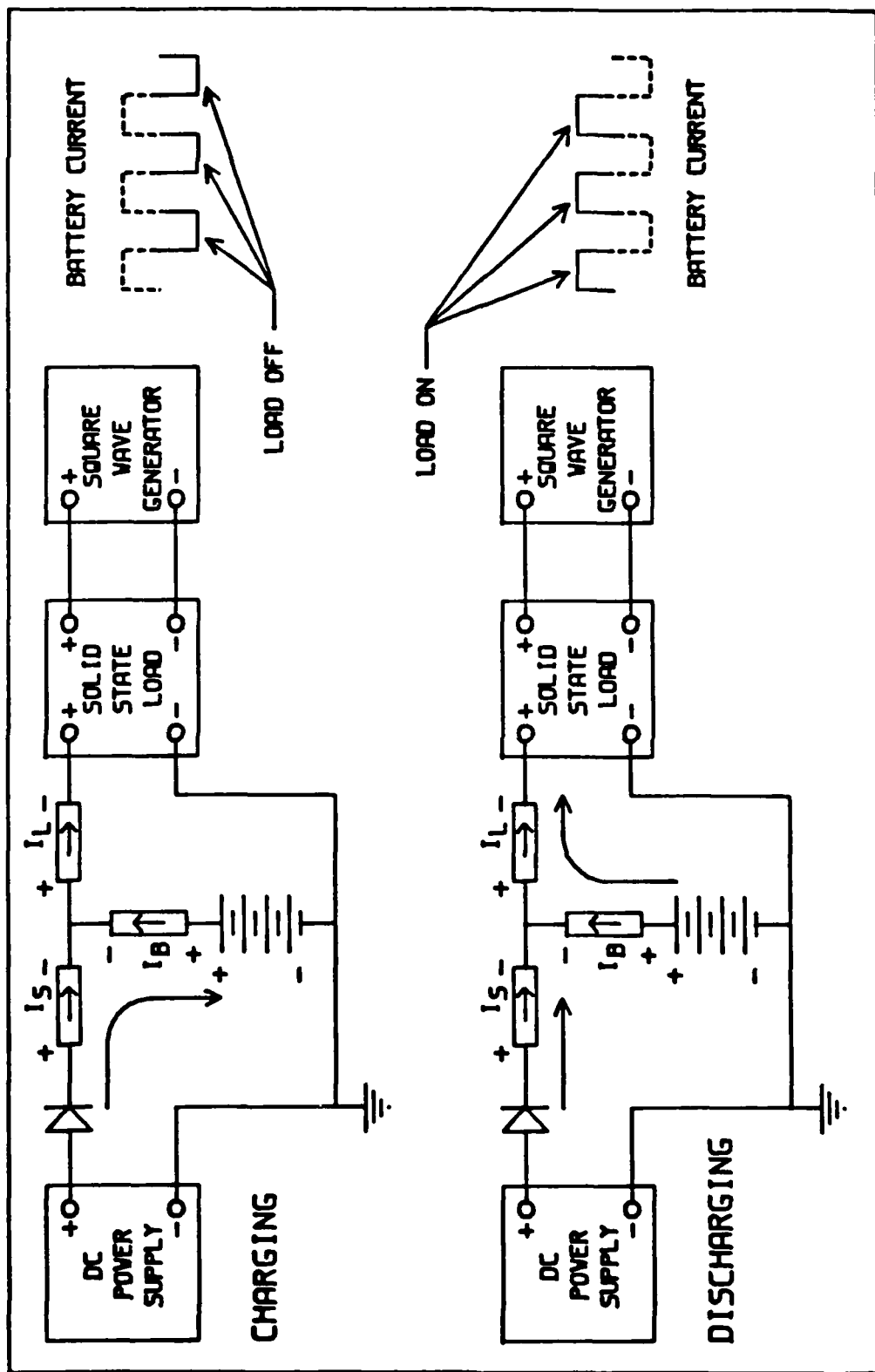
TEST CIRCUIT
FIGURE 4-2

29
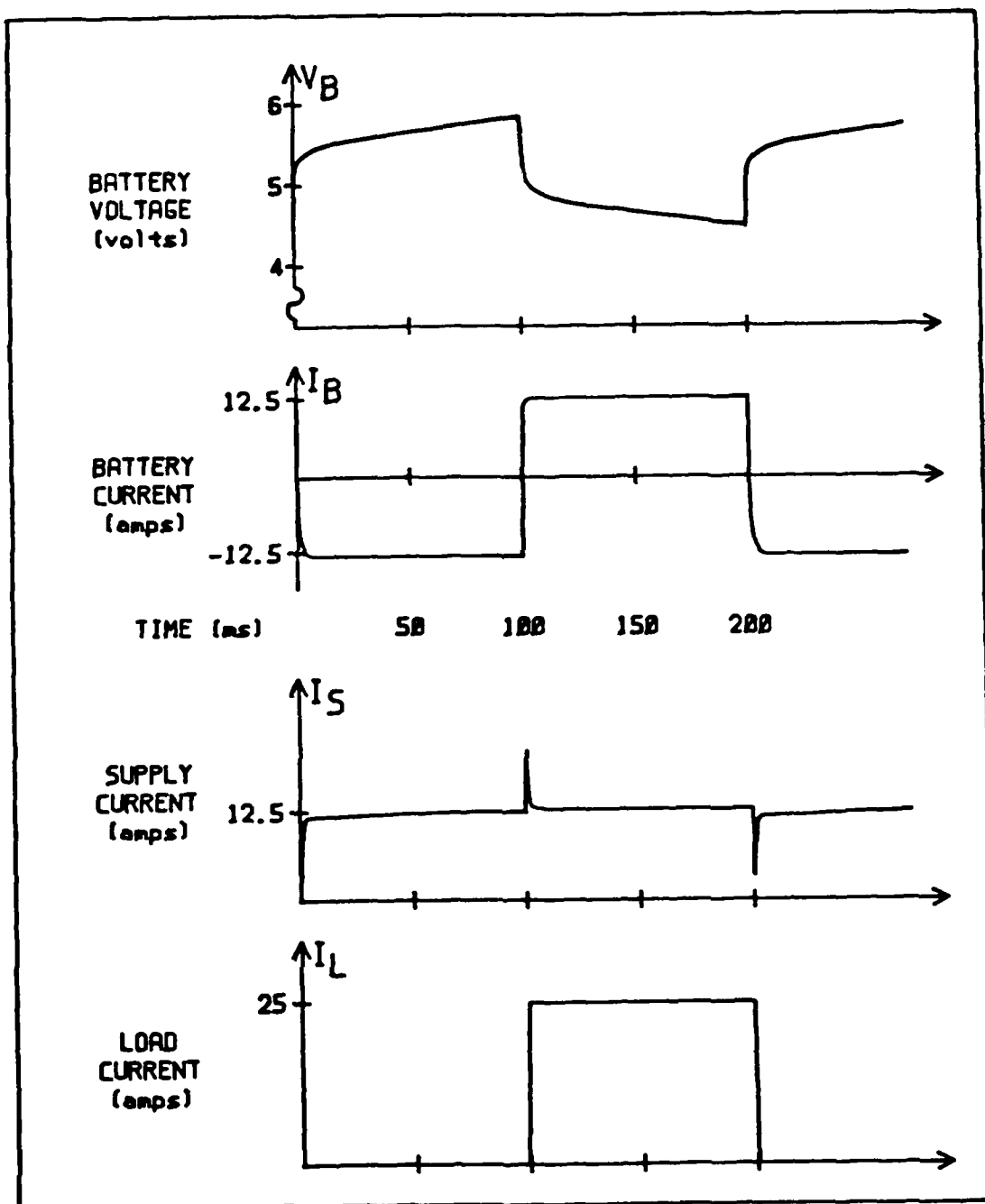
TYPICAL WAVEFORMS
FIGURE 4-3

Figure 4-3 shows typical voltage and current waveforms
from this test circuit.

30

Conditioning the Battery

Prior to testing the batteries, several charge/discharge cycles were completed to condition the batteries, stabilize their operation, and measure the initial capacity. The theoretical C rate of these pseudo bi-polar nickel-cadmium batteries was 1.4 amp-hours. The charging rate was 0.75 amperes for the first two cycles and then 1.5 amperes thereafter, until the total voltage reached 6.2 volts (1.55 volts/cell).

The battery was then discharged at a 1.0 ampere rate to a total voltage of 4 volts, or until any cell voltage was less than 0.5 volts. This cycling continued until the capacity was stable for two sucessive cycles. The measured capacity of each battery, after the initial conditioning cycles and after any additional testing, is shown in Table 4-1.

Since this experiment used a novel battery design, which did not have any demonstrated cycle life, the first series of tests were run under the same conditions (room temperature, 5 hertz cycle rate, 0.013% DOD) as Bishop and Stumpff's test [5]. This provided a relative comparison of battery types, which should be relatable to exixting documented cycle life test data from NWSC CRANE [13].

TABLE 4-1
MEASURED BATTERY CAPACITY (ampere hours)

BATTERY NUMBER	INITIAL CAPACITY	FINAL CAPACITY
1	0.1	0.0 (INTERCELL SHORT)
2	0.8	0.0 (INTERCELL SHORT)
3	1.0	0.8
4	0.95	0.93
5	0.63	NOT TESTED
6	NOT USED (INTERCELL SHORT)	
7	0.75	1.01

Energy Density Testing

Before starting the cycle and energy density testing, the batteries were charged at a 1.0 ampere rate for 30 minutes, so that the batteries would operate near the middle of their capacity range. This allowed some test equipment drift, without pushing the battery to either a fully charged or discharged condition.

The first series of tests were each 33.3 minutes long, operating the battery for 10,000 cycles at a 5 hertz rate. The primary purpose was to observe the battery operation at various DOD's and try to establish a maximum energy density at which the battery could operate for long periods of time without overheating.

Cycle Life Testing

To test the cycling life of the nickel-cadmium bat-teries, two 10^7 cycle continuous tests were run. The first was run with a charging current of 6.36 amperes and a load current of 13 amperes, running the battery at the same level (DOD of 0.013%) as Bishop and Stumpff. To determine if the test batteries were an improved design, a capacity check was completed, comparing the remaining capacity to that recorded by Bishop and Stumpff. The final 10^7 cycle test was run at a higher charging current of 12.5 amperes, 0.025% DOD, and load current of 25 amperes. A capacity check of each bat-tery was performed again, after completing the test.

Equivalent Circuit Capacitance

To calculate the effective double layer capacitance of the batteries and compute the internal equivalent voltages and resistances, voltage and current measurements were com-pleted both with and without the power supply connected to the circuit. One of the problems encountered and recognized by Bishop and Stumpff was the discharge of the power supply capacitors as the load cycled on, masking the true battery behavior. Removing the power supply before these tests eliminated this problem, allowing the measurement of current and voltage from the battery alone, when a step change of load current was applied to the battery.

V - Results and Discussion

Construction Problems

One of the major problems encountered during this test was the construction of the pseudo bi-polar battery. This problem fell into two general areas. First, sealing the electrolyte in a cell and second, insuring a satisfactory mechanical and electrical connection between the electrodes and the nickel intercell connector. Appendix A contains details of the problems and solutions.

Energy Density

The first objective was to increase the energy density of the battery used as a capacitive filter. Energy density is a function of the current through the battery (the voltage is nearly constant) and the weight of the battery. A description of the equivalent weight used in these energy density calculations appears in Chapter 4. A five hertz test was run at various charge and discharge currents starting at five amperes and increasing in five ampere steps. Each current level was maintained for 10,000 cycles with data collection occurring after approximately 5000 cycles.

Battery 4 was tested up to 25 amperes or a 18 C rate. By incorporating a larger load, Battery 7 was tested to 35 amperes, or 21 C. At this point, the exterior case reached 60°C and further increases were not attempted. The 60°C cutoff was an arbitrary level picked to insure internal

34

temperatures would remain well below the boiling point of the electrolyte, approximately 100°C.

The resulting battery voltage and current plots were utilized to evaluate the average capacitance during discharge, the energy density, and efficiency of the battery.

To calculate the energy into and out of the battery and average capacitance during discharge, the battery voltage was assumed to be a step increase/decrease followed by a linear ramp. The average ramp voltage was used as a constant value for the entire charge or discharge. The initial step change was due primarily to the internal instantaneous series resistance of the battery. The remaining ramp change was primarily a function of the double layer capacitances and faradaic discharge. Since the solid state loads and power supplies are not ideal devices, the battery was not reacting to a perfect step increase or decrease in current during the first few milliseconds of any half cycle. Therefore, the calculations started after the load and power supply currents had stabalized, i.e., approximately one millisecond after the start of the load switching.

Figure 4-3 showed a typical waveforms from the test circuit. The voltage rate of change varied from about 9 volts/second during the first 20 milliseconds to 3 volts/ second for the remaining 80 milliseconds. From Figure 4-3, the average voltage, using a straight line approximation, is

35

4.90 volts, while the integral of the voltage divided by the time gives an average of 4.86 volts. This approximation results in less than a 1 percent error.

Figures 5-1 through 5-3 depict the average capacitance, energy density, and efficiency as functions of DOD. At the higher current levels examined with Battery 7, it was observed that as battery voltage varied, so did the other parameters, particularly average capacitance. For example, at 30 amperes discharge current the end of the discharge voltage dropped below 4 volts. By increasing the average battery voltage from 5.1 to 5.3 volts, this low point was raised to approximately 4.25 volts, roughly the value recorded during the 25 ampere discharge test. This point coincides with the abrupt reversal of the average capacitance and efficiency in Figures 5-1 and 5-3. At the highest current, the test battery's equivalent energy density was over 40 joules per pound! In addition, it appears that battery discharge voltage has a significant effect on the voltage regulation, or effective average capacitance, and efficiency.
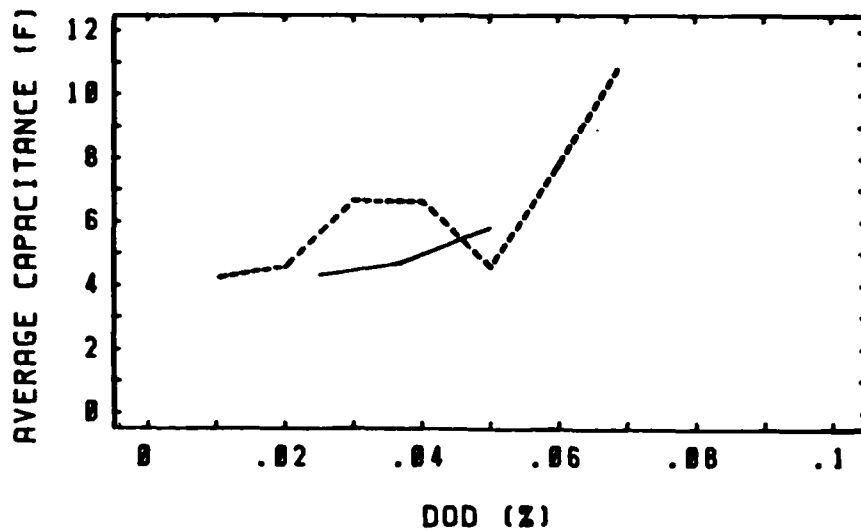
AVERAGE CAPACITANCE VERSUS DOD
FIGURE 5-1
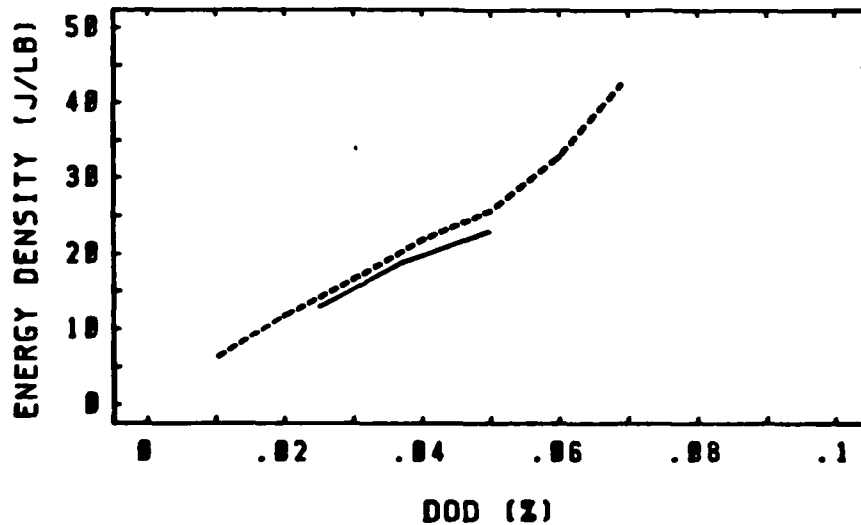
ENERGY DENSITY VERSUS DOD
FIGURE 5-2
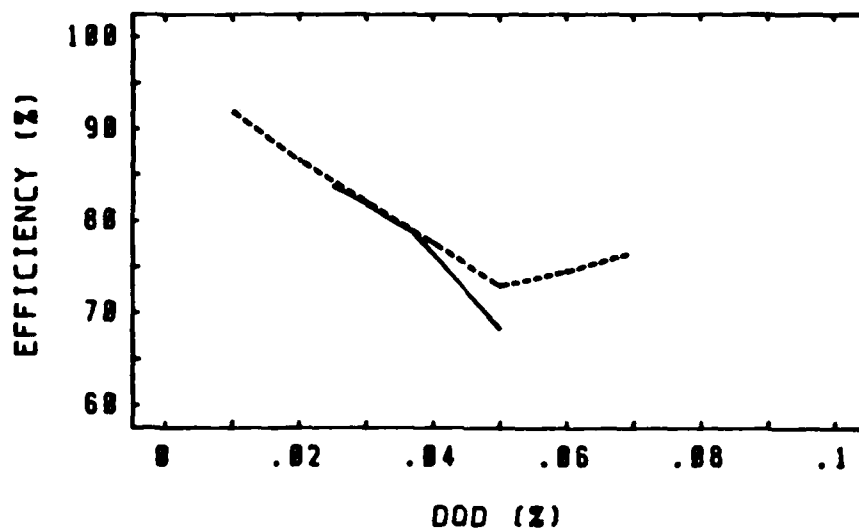
37

EFFICIENCY VERSUS DOD
FIGURE 5-3

Cycle Life

In order to project a possible cycle lifetime for the new design, two batteries were run for 10^7 cycles. Since this is only a small fraction of the proposed lifetime and no catastrophic failures occurred, no conclusive data was obtained. Figures 5-4 through 5-8 show average battery voltage, energy density, average capacitance, efficiency, and capacity versus cycles completed at DOD's of 0.013% and 0.025%. These DOD's, which reflect the depth of capacity discharged each cycle, not necessarily the actual state of charge, were based on the theoretical battery capacity, not the rated capacity.

38

The relatively low measured capacity, when compared to the theoretical capacity, may be due to incomplete conditioning of the batteries prior to testing. However, the main purposes of these tests were demonstrate energy densities above 10 Joules/pound, document performance of the batteries over 10^7 cycles, and analyze the battery influence on voltage and current when used as a filter. Incomplete conditioning did not noticeably impede any of these objectives.

There was only one possible failure during the 10^7 cycle test. After approximately 4.8 million cycles, Battery 3 started to discharge. This discharge occurred over a weekend and was not discovered for approximately 27 hours. By that time the average battery voltage had dropped to 3.25 volts. The voltage variation during cycling dropped below the recorder's range and was unmeasurable. However, the battery continued to supply 6.4 amperes to the load, though at a lower voltage. The decrease in battery voltage was a result of the battery operating a very low state of charge. The load had increased its current required, which led to the gradual discharge of the battery, After two reconditioning cycles on the battery, the capacity was measured at 0.98 ampere/hours, only a 5% drop from its precycling capacity. The cycling test was then continued on the battery to complete 10^7 cycles.
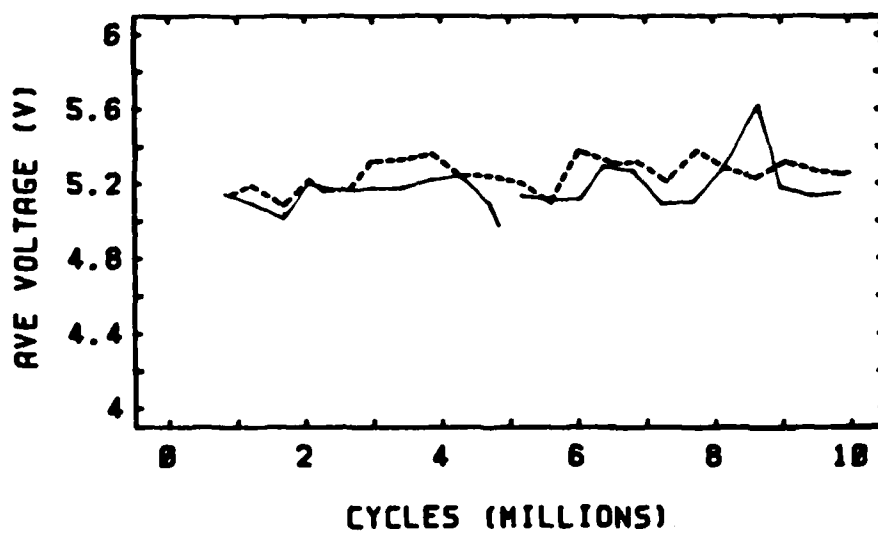
AVERAGE BATTERY VOLTAGE VERSUS CYCLES
FIGURE 5-4
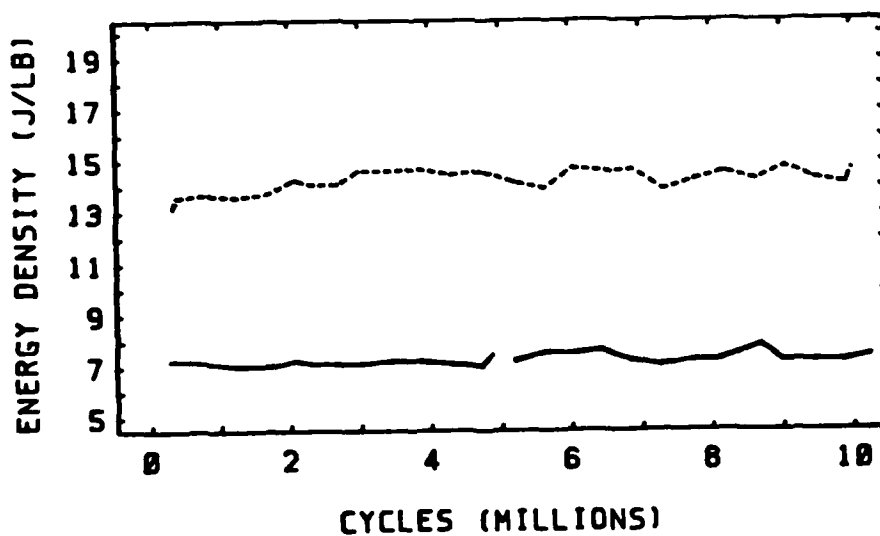
ENERGY DENSITY VERSUS CYCLES
FIGURE 5-5
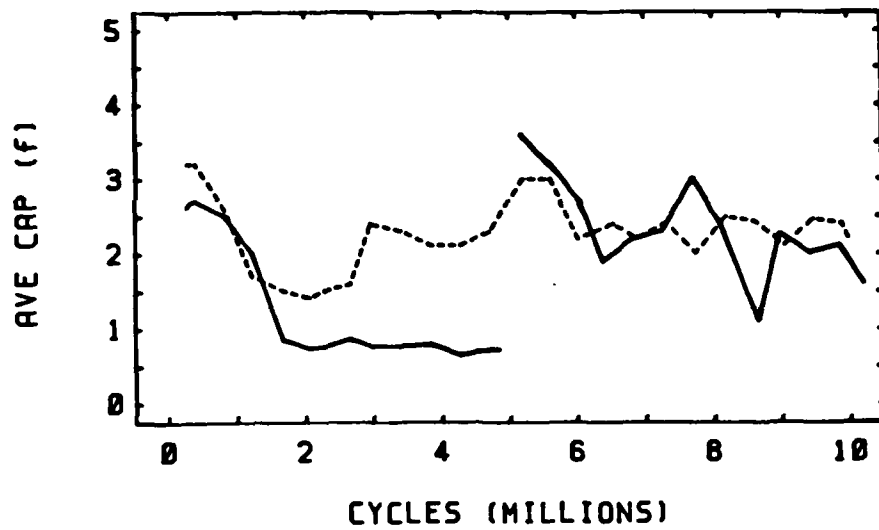
AVERAGE CAPACITANCE VERSUS CYCLES
FIGURE 5-6
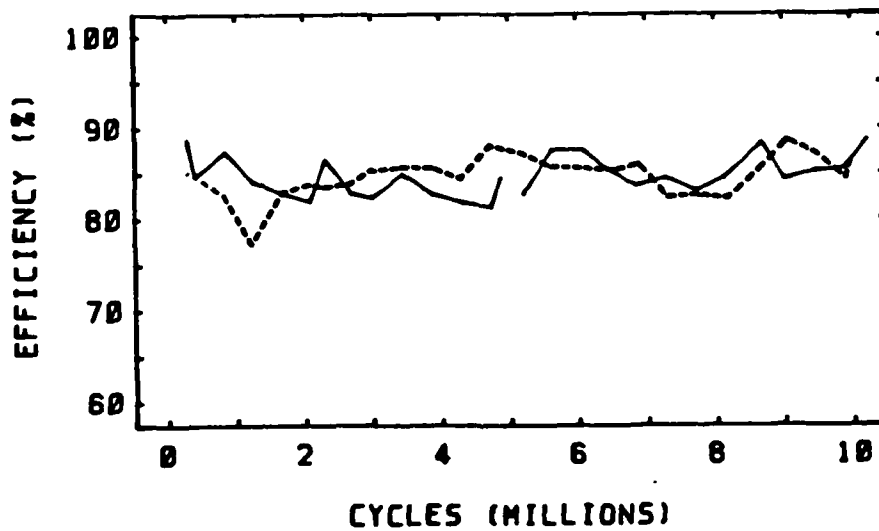
EFFICIENCY VERSUS CYCLES
FIGURE 5-7

41
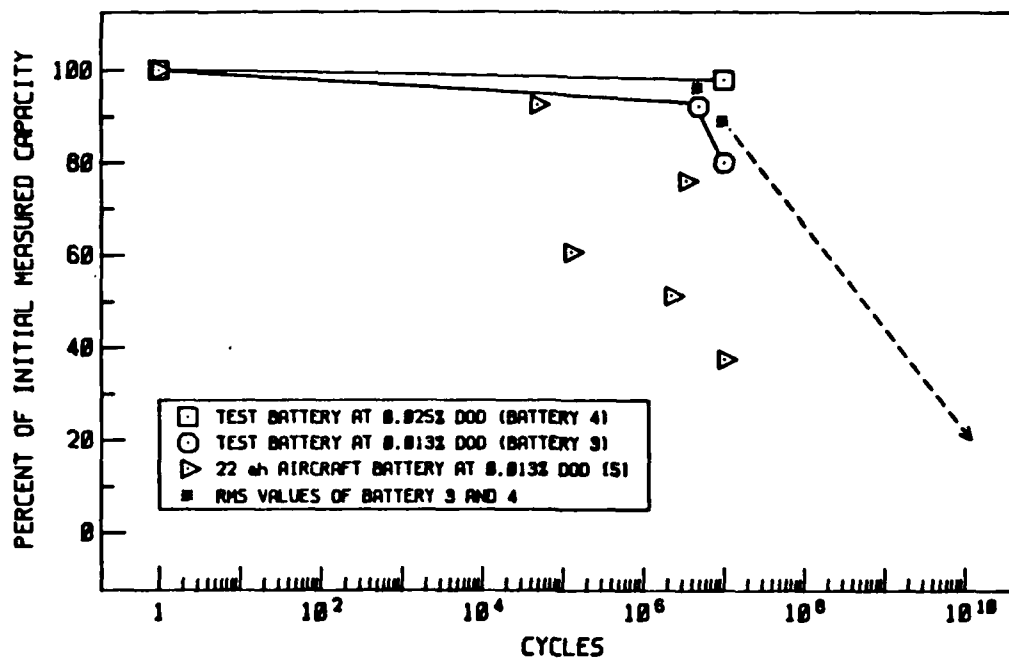
PERCENT CAPACITY REMAINING VERSUS CYCLES
FIGURE 5-8

Although not a failure, Battery 3 had a varying internal resistance during the 10^7 cycle test. It was found that by increasing pressure on the end of the battery, the internal resistance would drop. After completing the testing, the battery was taken apart. In addition to the broken weld during construction, several other welds were very easy to break during dissection of the battery after testing. The varying internal resistance is attributed to the poor welds.

Figure 5-8 shows the relative capacity of the test batteries before and after cycling. Battery 3 was reconditioned around 4.8 million cycles and therefore has three data points. As a comparison, the relative capacity measured by Bishop and Stumpff [5], from their test of 5 series

42

connected 22 ampere/hour nickel-cadmium aircraft type cells is also included in Figure 5-8.

After completing the 10^7 cycle test, Battery 3 was dissected and samples of both electrode types were examined. Photographs of these electrodes are contained in Appendix D. There was no apparent change in the nickel electrode. The cadmium electrode, however, showed a significant change. After the cycling there were no large cadmium crystals left, only small ones, about 500 times smaller than those crystals from an uncycled electrode. It is possible that the cadmium electrode may be the lifetime failure mechanism, typical of nickel-cadmium batteries in "normal" operations. Since most nickel-cadmium batteries are designed to be nickel electrode capacity limiting, this decrease would not show up until the cadmium capacity dropped below that of the nickel electrode. Post cycling capacity testing confirmed this for Battery 3.

Figure 5-8 shows the measured battery capacity versus number of cycles completed at a 5 hertz rate. Assuming that any decrease in measured capacity is attributable to a cadmium loss, the abrupt change in Battery 3's capacity could be attributed to the gradual failure of the cadmium electrode, which finally dropped below that of the nickel electrode. Bishop and Stumpff's batteries also show a fairly rapid decrease in measured capacity after about 5 million cycles, which may have also been a result of cadmium electrode erosion.

43

Even with this increased rate of capacity loss, these batteries appear to have lifetimes of 10^9 cycles or more. The dashed line in Figure 5-8 runs through the RMS values obtained from Batteries 3 and 4 at 5×10^6 and 10^7 cycles. It projects approximately a 50% remaining capacity at 10^9 cycles. Projecting this line back towards 1 cycle, results in a value of approximately 250% of initial battery capacity. This is roughly equivalent to about 80% of the initial theoretical cadmium capacity. However, there are still too few data points to accurately predict the lifetime of batteries when used as filters.

There were no identifiable trends or failures in energy density, average capacitance, or efficiency during the 10^7 cycles. Figures 5-4 through 5-7 only show the trends of these values through 10^7 cycles. Unless a catastrophic failure occurs, such as a complete short or open circuit, end of life performance criteria, such as effective average capacitance or efficiency, will have to be established before further testing can project an actual lifetime for these batteries when used as filter elements.

Equivalent Circuit

The third area of interest was to determine what effect a battery would have in a circuit when used as a filter element. During the energy density and 10^7 cycle testing, the power supply current was not constant. It appeared that the power supply output capacitors were charging and dis-

44
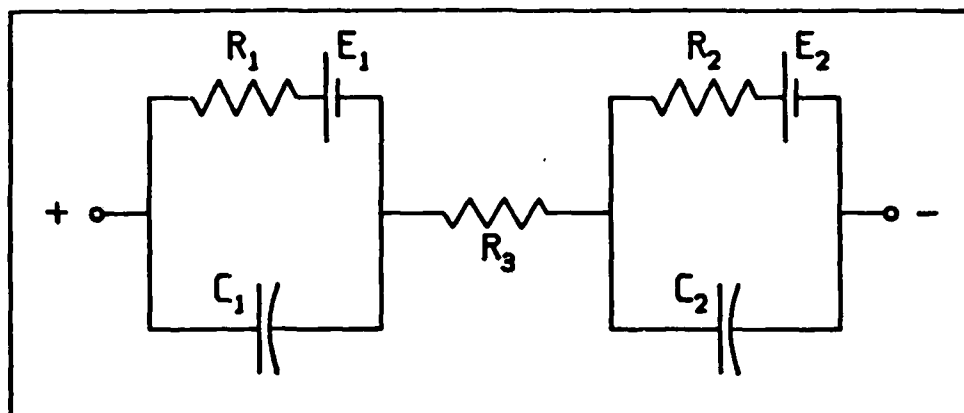
NEW NICKEL CADMIUM CELL EQUIVALENT CIRCUIT
FIGURE 5-9

charging faster than the battery during the first millisecond after the load switched on or off. To eliminate as many variables as possible, the battery was charged and then connected directly to the load without a power supply. The resulting voltage and current waveforms, together with those obtained during earlier testing, were used to modify the electrical equivalent circuit of Figure 2-2.

Figure 5-9 shows the proposed new equivalent circuit. The voltage source was split into two elements corresponding to the voltage across each electrode/electrolyte interface. R_1 and R_2 are the nickel and cadmium electrode/electrolyte ionic and activation resistances respectively. C_1 and C_2 are the double layer capacitances and R_3 is the ohmic resistance through the electrolyte and electrode tabs.

Each electrode had a volume of approximately 3.55 cm^3. Using a nickel Brunauer, Emmett, and Teller (BET) surface area to volume ratio of 70 m^2/cm^3, and a cadmium BET surface

45
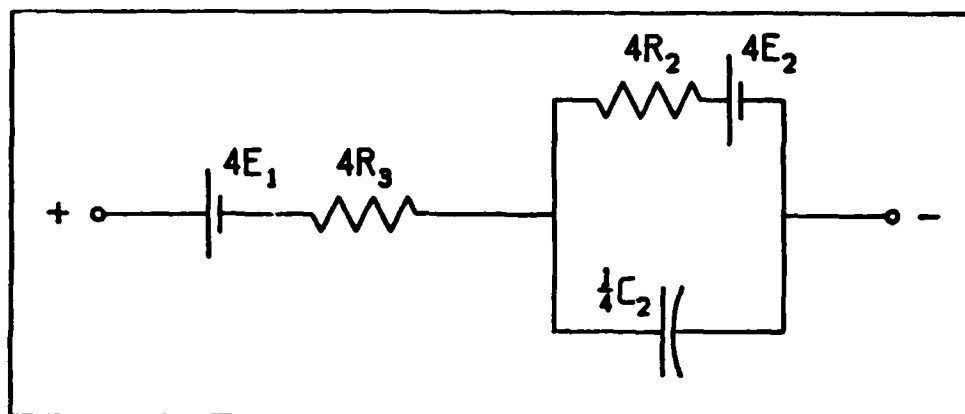
SIMPLIFIED NICKEL CADMIUM BATTERY EQUIVALENT CIRCUIT
FIGURE 5-10

area to volume ratio of 6 m^2/cm^3 [12], the theoretical
double layer capacitances were calculated. The nickel dou-
ble layer capacitance is approximately 5000 farads and the
cadmium double layer capacitance is approximately 11 farads.

The change in voltage due to the faradaic discharge for
the batteries at 5C for 0.1 seconds at a 50% state of charge
is approximately 0.14 millivolts. This term was neglected
since it was over 1000 times less than observed voltage
changes. Most of the discharge, then, would appear to be
across the cadmium capacitances since they are over 100
times smaller than the nickel capacitances.

Revising Figure 5-9 and combining 4 cells in series
gives the simplified battery equivalent circuit shown in
Figure 5-10. E_1 is the combination of the nickel electrode
voltage, resistance, and double layer capacitance. R_3 is
still the series ohmic resistance and C_2, E_2, and R_2 repre-
sent the cadmium electrode.

46

The equivalent circuit of Figure 5-10 results in an equation for the total battery voltage of:

$$V(t) = E_o - 4iR_3 - 4iR_2[1 - \exp(-t/R_2C_2)] \qquad (7)$$

where

$V(t)$ = Total Battery Discharge Voltage over time

E_o = Initial Voltage before Discharge

i = Total Discharge Current

t = Time of Discharge

R_2 = Cadmium/KOH Ionic Activation Resistance

R_3 = Series Electrolytic Ohmic Resistance

C_2 = Cadmium Double Layer Capacitance

From battery voltage curves, $4R_3$ was between 20 and 57 milliohms for Battery 3 and 28 to 38 milliohms for Battery 4. Taking the initial rate of change of voltage from the discharge voltage waveform obtained during the early part of the 10^7 cycle test and using equation (5), $(1/4)C_2$ was approximately 0.3 farads. After the 10^7 cycle test, it was not possible to determine C_2, although it appeared to have decreased significantly.

After determining $4R_3$ from the instantaneous change of voltage at both the beginning and end of the discharge, $4iR_2$ was assumed to be the remaining voltage drop occurring during the discharge. Solving for $4R_2$ gave a value of approximately 54 milliohms for both Battery 3 and 4.

DISCHARGE CURRENT: 6.3 AMPS
(4.5 C RATE)

□ EXPERIMENTAL VALUES
— THEORETICAL CURVE
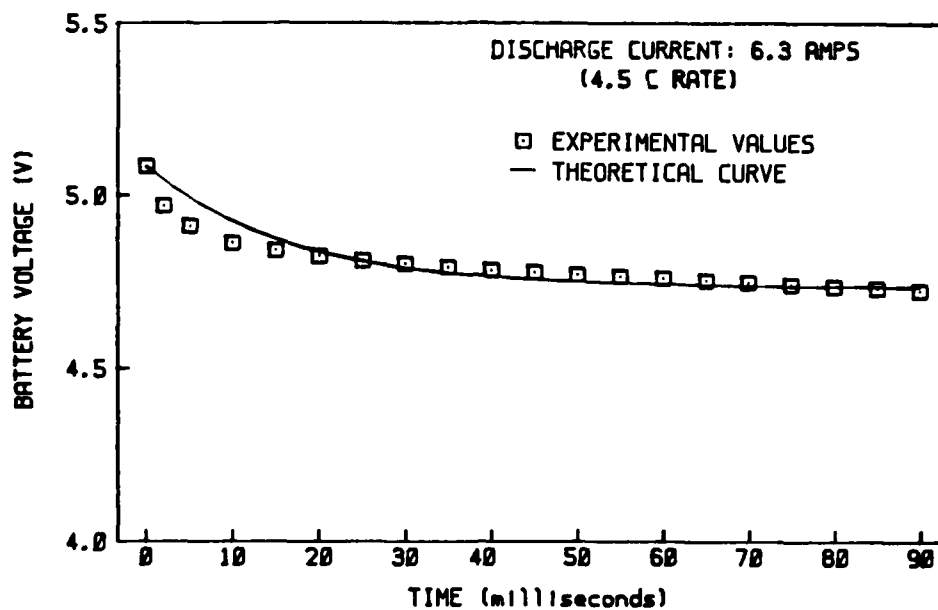
BATTERY 3 DISCHARGE VOLTAGE
FIGURE 5-11

DISCHARGE CURRENT: 6.3 AMPS
(4.5 C RATE)

□ EXPERIMENTAL VALUES
— THEORETICAL CURVE
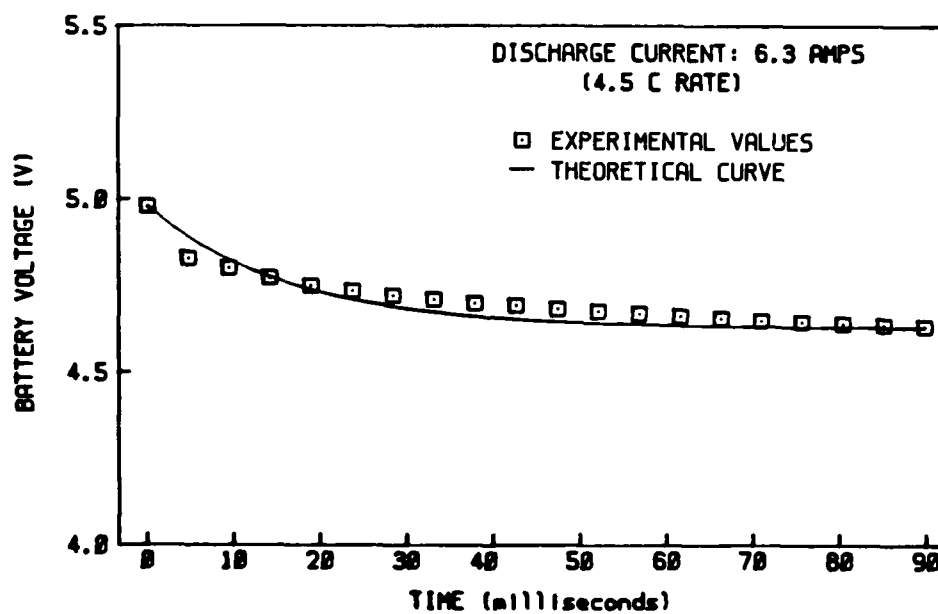
BATTERY 4 DISCHARGE VOLTAGE
FIGURE 5-12

48

DISCHARGE CURRENT: 6.3 AMPS
(4.5 C RATE)

□ EXPERIMENTAL VALUES
— THEORETICAL CURVE
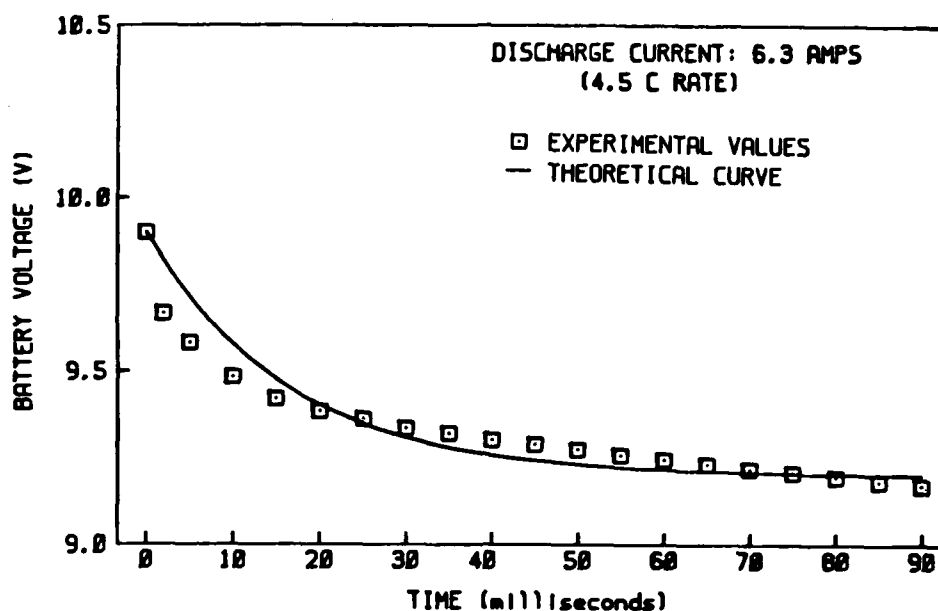
BATTERY 3 + 4 DISCHARGE VOLTAGE
FIGURE 5-13

Using these values and equation (7), V(t) was plotted against the actual voltage waveforms for Battery 3 and 4 as shown in Figures 5-11 and 5-12. Figure 5-13 shows the calculated V(t) and actual voltage of Batteries 3 and 4 connected in series. The equation for V(t) then became:

$$V(t) = E_o - 8iR_3 - 8iR_2[1 - exp(-t/R_2C_2)] \qquad (8)$$

The same values obtained before for C_2, R_2, and R_3 were used as well as the measured current and initial voltage. This verifies that the equivalent circuit in Figure 5-10 appears to be reasonable approximation for these batteries when used as a capacitive filter.

When running the maximum energy density test with Battery 7, the voltage and current waveforms were recorded to

evaluate the equivalent circuit of Figure 5-10. Appendix D contains oscilloscope pictures of these waveforms. However, the values obtained for R_2, R_3, and C_2 varied as the discharge current and battery voltage varied. $4R_2$ ranged from 12 to 40 milliohms, $4R_3$ ranged from 18 to 35 milliohms, and $(1/4)C_2$ varied from 0.14 to 1.66 farads. It also appeared that at discharge currents above 10C that the nickel double layer capacitance could no longer be ignored. Further analysis of this, which would appear to involve a more complex equivalent circuit, was beyond the scope of this paper.

As the number of cycles on the batteries increased, the voltage curve became initially steeper and then flatter, suggesting that the cadmium double layer capacitance may be decreasing. This may be attributed to the breakdown of the cadmium causing the electrode surface area to decrease.

If this is the case, a more uniform voltage output, excluding the first 5 milliseconds or so of each pulse, may be obtained by conditioning the battery, causing the cadmium capacity and capacitance to decrease. The nickel double layer and faradaic capacitances would then dominate (after the first 10 milliseconds) giving a much higher effective capacitance over the discharge cycle for the battery. However, this will leave a larger rate of change of voltage at the beginning of each discharge period, possibly allow the battery to become cadmium electrode capacity limited more quickly, and possibly reduce the battery lifetime.

50

Discharge Without Power Supplies

To minimize test circuit induced stray inductance and capacitance on the waveforms of the battery while cycling, the power supply was disconnected. The battery was then connected directly across the load with a minimum of test circuit wiring. The resulting waveforms showed that the test circuit induced inductance was minimal, but the power supply capacitors charged and discharged during the first millisecond of each load change. This caused the power supply current to fluctuate so that the battery was not required to supply an instantaneous change in current. After the first millisecond the power supply and load currents were essentially constant. Therefore, analysis starting after one millisecond is accurate, even with the power supply connected to the battery. Appendix D shows a typical waveform showing the power supply current and battery current as the load cycled on.

VI - Conclusion and Recommendation

Conclusion

This investigation consisted of several tests of specially fabricated nickel-cadmium batteries having circular disk type electrodes. These tests addressed three areas. First, would the circular electrodes increase the maximum energy density when compared to standard aircraft batteries. Secondly, what energy density could be maintained and achieve a lifetime of 10^9 cycles at 5 hertz. And finally, how does the battery influence the voltage and current waveforms to the load.

The advantage of a bi-polar battery is its extremely low internal resistance and inductance, enabling it to deliver pulses of high current for short periods. Reducing the internal losses lead to greater efficiency and increases the potential for a higher energy density. This reduction is achieved in part, by straightening and shortening the current path within the battery.

Bi-polar electrodes have been constructed at a number of facilities, however, the fabrication of a bi-polar battery has been complicated by the lack of a reliable edge seal to prevent electrolyte shorting between cells. In order to take advantage of the bi-polar geometry without inheriting the edge seal problems, a battery with a short current path was designed specifically for use in this

project. It consisted of a stack of four single cell button style batteries in which adjoining cells shared a common wall and intercell connector. A circular electrode with a large central current tab to uniformly collect the current was selected. A neoprene O-ring placed around a nickel slug was inserted in the plexiglas intercell wall, providing a electrical current path and electrolytic seal between cells.

With the voltage constant, energy density is a function of the current through the battery and the weight of the battery. A 5 hertz test was run at various charge and discharge currents from 5 to 35 amperes (up to 21 C). Each current level was maintained for 10,000 cycles. At the 21 C rate the exterior case reached 60°C and further increases were not attempted. At the highest current, the test battery's equivalent energy density was over 40 joules per pound. In addition, it appears that the battery discharge voltage has a significant effect on the voltage regulation, on effective average capacitance, and efficiency.

Two batteries were run for 10^7 cycles each. Since this is only a small fraction of the proposed lifetime and no catastrophic failures occurred, no conclusive data was obtained. After completing the test, samples of both electrode types were examined. There was no apparent change in the nickel electrode. The cadmium electrode, however, showed a significant change. It is possible that the cadmium electrode may be the lifetime limiting failure mecha-

53

nism. Even with the increased rate of capacity loss, above about 5 million cycles, these batteries appear to have lifetimes of 10^9 cycles or more at a 5 hertz rate.

No identifiable trends or failures in energy density, average capacitance, or efficiency were observed. Unless a catastrophic failure occurs, such as a complete short or open circuit, end of life performance criteria, such as effective average capacitance or efficiency, will have to be established before further testing can project an actual lifetime for these batteries when used as filter elements.

The equivalent circuit of Figure 5-10 gave a simple analysis of the battery's operation. The leading edge of the current pulse, and voltage output from the nickel-cadmium battery is shaped by its short term or transient characteristics. These characteristics are dominated by the battery's double layer capacitance and internal resistance. For these tested batteries, R_2 varied between 3 and 13 milliohms, R_3 varied between 5 and 16 milliohms, and C_2 ranged from 0.56 to 6.64 farads. Using equation (7), the calculated battery discharge voltage correlated well for Batteries 3 and 4 seperately, and Batteries 3 and 4 in series. However, the values varied as the discharge current and battery voltage varied and further analysis appears to involve a more complex equivalent circuit, which was beyond this paper.

54

As the number of cycles on the batteries increased, the voltage curve became initially steeper and then flatter. This suggests that the cadmium double layer capacitance was decreasing, supporting the conclusion that cadmium electrode breakdown may be the lifetime limiting failure mechanism.

Test circuit induced inductance was minimal, but the power supply capacitors charged and discharged during the first millisecond of each load change. This caused the power supply current to fluctuate so that the battery was not required to supply an instantaneous change in current. After the first millisecond, the power supply and load currents were essentially constant. Analysis starting after one millisecond is accurate even with the power supply connected to the battery.

In summary, a maximum equivalent energy density of over 40 joules per pound was demonstrated by the specially con-structed test nickel-cadmium batteries. Ten million cycles at a 5 hertz rate with a useful equivalent energy density of 14 joules per pound were completed. Capacity degradation was negligible for one battery and only a 20% decrease for the other. Cadmium electrode failure may be the factor limiting lifetime. An equivalent circuit was derived, but further testing will be required to completely evaluate the results. Internal resistances and double layer capacitances varied with changes in either battery voltage or current,

suggesting that a more complex equivalent circuit may be required.

Recommendations

The use of batteries as filter elements for repetitive pulsed loads for long periods of time is a new and unproven concept. Before funds can justifiably be allocated to large scale research, some understanding of the battery's ability to accomplish this task must be obtained. This information can then be used to determine what, if any, areas warrant further investigation. This study has provided this initial information. Based on the high energy density obtained, as compared with capacitors, the relatively high effective capacitance of the battery, the clean response to the load, and the trend towards long life the following recommendations are made:

1. At the earliest opportunity, begin a long term life cycle test, 10^8 cycles or more, to obtain more conclusive data on the battery's long term capability to fucntion as a filter element.

2. Construct a bi-polar battery, if necessary achieving an intercell seal at the expense of weight, to determine if a bi-polar design would significantly improve the electrical characteristics desired. If successful, this would support large scale efforts to achieve a true lightweight bi-polar design.

3. Begin more detailed experimentation to investigate the relationships between SOC, DOD, energy density, efficiency, output response, average voltage, and average effective capacitance to identify optimum operating conditions and devise a control system to maintain those conditions.

4. Finally, in view of the dramatic change in the cadmium structure, further analysis is needed to identify exactly what changes are taking place in the electrode and how these changes will effect the long term performance of the battery when used as a voltage filter element.

Appendix A - Test Battery Fabrication

Overview

Several four-cell pseudo bi-polar batteries were built. Construction techniques were adjusted to improve battery performance as experience was gained. Figure A-1 displays various views of the battery including an expanded side view which establishes the relative position of the parts. This view is repeated in Figures A-2 through A-5 which describe each of the components in detail.

Case

The case was bored from solid plexiglas stock. Figures A-2a and A-2b illustrate this piece. The interior steps or ridges position the cell walls during construction. Standard 5 to 8 psi relief valves, or vents, are located across the top of the case.

The vent sockets also serve as refill ports to maintain proper electrolyte levels. The reference electrode holes are also spread across the top of the case. These holes accommodate one millimeter cadmium wire. The stand is a simple plexiglas rack to support the entire assembly.

Cell Walls

The cell walls were cut from a 0.187 inch thick plexiglas sheet to the various diameters specified in Figure A-3. The ridge in the center hole locates the proper position of

the intercell electrical connector (nickel slug), just as the ridges in the case serve to position the walls.

Intercell Electrical Connector

These pieces are detailed in Figure A-4. They were cut from a solid nickel sheet 0.210 inches thick.

Electrodes

The physical dimensions of the electrodes are depicted in Figure A-5. The positive nickel and negative cadmium electrodes were cut to the same specifications. Initial supplies of electrodes were manufactured by Eagle Picher Industries, Colorado Springs (part numbers PLP-434 and PLN-400). Locally manufactured electrodes were also coined and cut to these dimensions.

Actual Construction

The following construction steps were used on the initial batteries and form the basis for subsequent adjustments to improve battery performance by improving the assembly process.

1. The intercell electrical connector was fitted with a 1/16 inch thick stock neoprene rubber O-ring with an inner diameter of 1 inch. This O-ring/nickel slug combination was then pressed into the intercell walls.

2. The electrodes were then spot welded to the intercell connectors.

3. These assemblies were glued into the case one at a time

with dichloromethane. A layer of pellon separator and the reference electrode were placed in each cell as the layers were glued in place.

4. Finally the batteries were filled with electrolyte and the relief valves were screwed in place.

Refinement of Electrode Welding

During the gluing of Battery 2, one cadmium electrode to nickel slug weld was broken. Rewelding was not possible, so construction was completed by placing the electrode in its proper place and relying on the pressure of the next layer to hold it there.

On Batteries 4 through 7, the smooth side of a perforated nickel foil, typical nickel cadmium current tab material, was welded to both sides of the nickel slug before the electrodes were attached. The rough side of the tab was driven into the electrode's center area tab by the spot welder. The resulting weld connected the nickel wire within the electrode to the nickel tab material. This weld proved to be stronger. However, one nickel slug to foil weld was broken (Battery 3) during assembly.

Temperature readings of the end terminals and case of Battery 4 during the extended cycle test indicated that the nickel terminal was hotter than the case or cadmium terminal. This was attributed to higher current densities due to the few welds remaining intact. To improve this weld,

60

nickel electrodes with unimpregnated centers were produced for Battery 7. The nickel impregnation was accomplished using a modified Pickett electrochemical deposition process [14]. The impregnation solution was altered by deleting the alcohol since it only served to lower the solution boiling point [7].

Refinement of Plexiglas Gluing Techniques

During the operation of both Batteries 1 and 2, excessive intercell electrolyte leakage was detected. This was attributed to the cell-wall-to-battery-case glue joints. Subsequent batteries were leak checked as each cell was completed. This was accomplished by fitting a low pressure air line with a Tee. One end of the Tee was fitted with a typical relief valve and the other end was attached to the cell to be tested. The exterior seam was submerged in water and the cell was pressurized. The appearance of bubbles indicated the location of potential electrolyte leaks. Once detected these areas were reglued and the test repeated until the joint was air tight at the expected maximum relief valve pressure of 8 psi.

Electrolyte leakage was dramatically reduced in Batteries 3 and 4, however some intercell leaks persisted. The exterior of the cases of these batteries were polished, allowing direct viewing of the glue joints. This revealed areas where very little glue had penetrated between the case and the wall. All remaining cases were polished before

assembly. Gaps in the glue in Batteries 5 and 6 were attri-
buted to extremely tight fitting pieces. The case for
Battery 7 was rebored slightly to increase the gluing space.
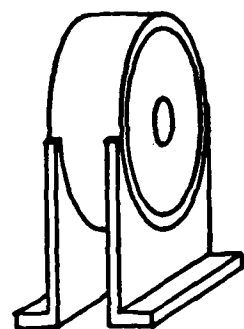
PERSPECTIVE
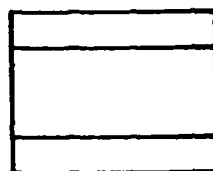
TOP VIEW
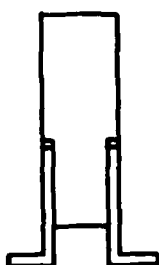
SIDE VIEW
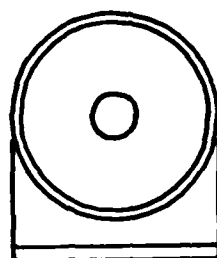
END VIEW
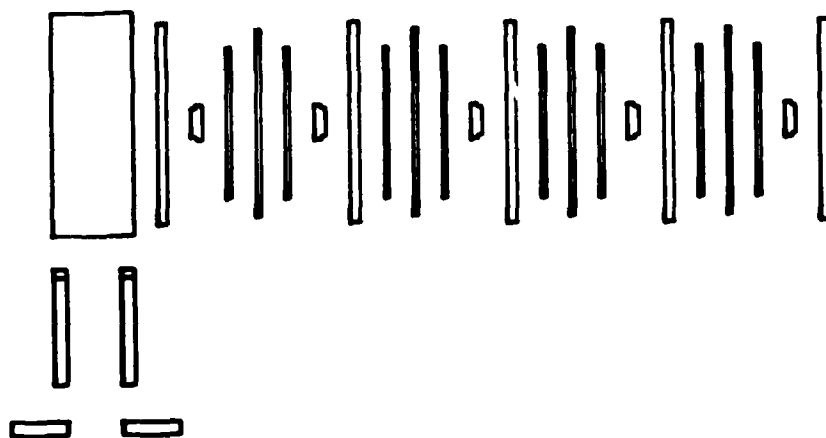
EXPANDED VIEW

FABRICATED TEST BATTERY
FIGURE A-1

63

1.517

2.00
2.13
2.16
2.19
2.22
2.25
2.50

0.312
0.270
0.270
0.270
0.270
0.125

MEASUREMENTS IN INCHES

BATTERY CASE
FIGURE A-2ₒ

64

SIZED AND THREADED
FOR RELIEF VALVE

GLUE/SEALER
DEPRESSION

← 0.070 →

SIZED FOR 1mm C_d WIRE

RELIEF VALVE SOCKET

REF. ELECTRODE HOLE

0.270

0.270

0.270

0.357

EXPANDED
VIEW

15° 15° 15°
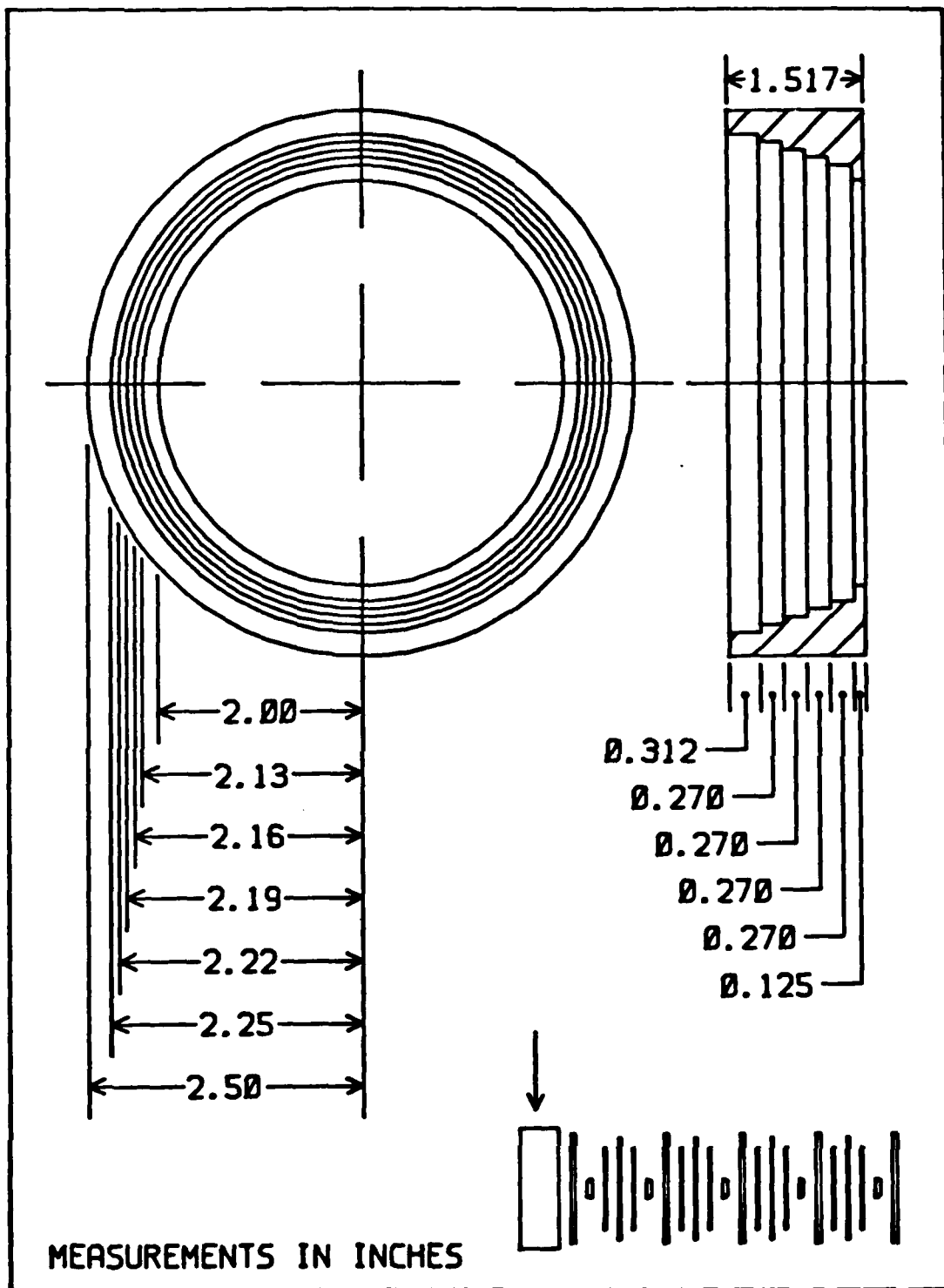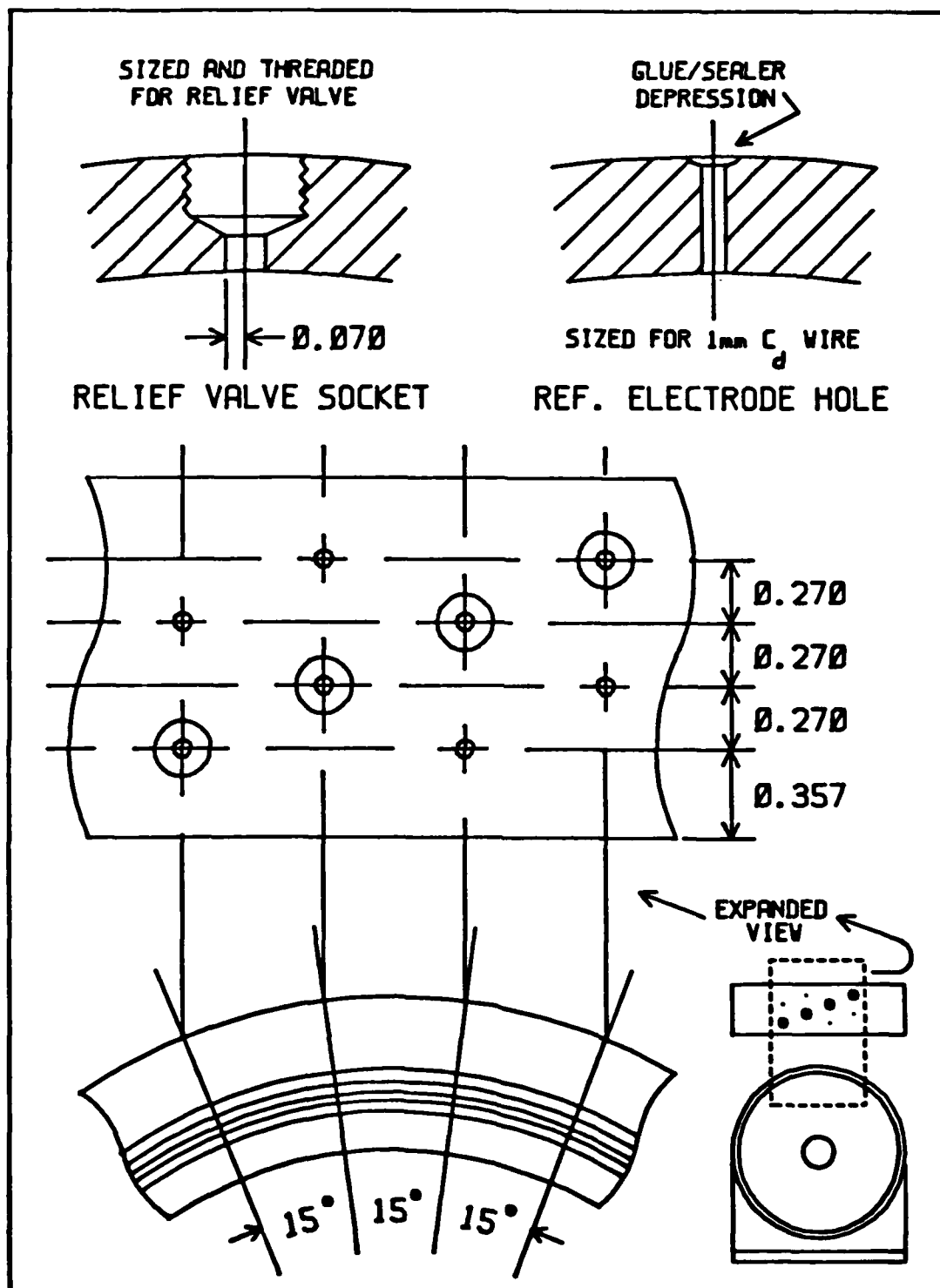
CASE (RELIEF VALVE AND REF. ELECTRODE LOCATIONS)
FIGURE A-2b

0.187

0.136

0.051

0.545
0.625

R

MEASUREMENTS IN INCHES

PIECE	R
a	2.130
b	2.160
c	2.190
d	2.220
e	2.250

CELL WALLS
FIGURE A-3

0.210

0.50
0.545
0.625

0.055
0.0625
0.030
0.0625

0.01375

RADIUS=0.03125

0.08625

O-RING SLOT

MEASUREMENTS IN INCHES
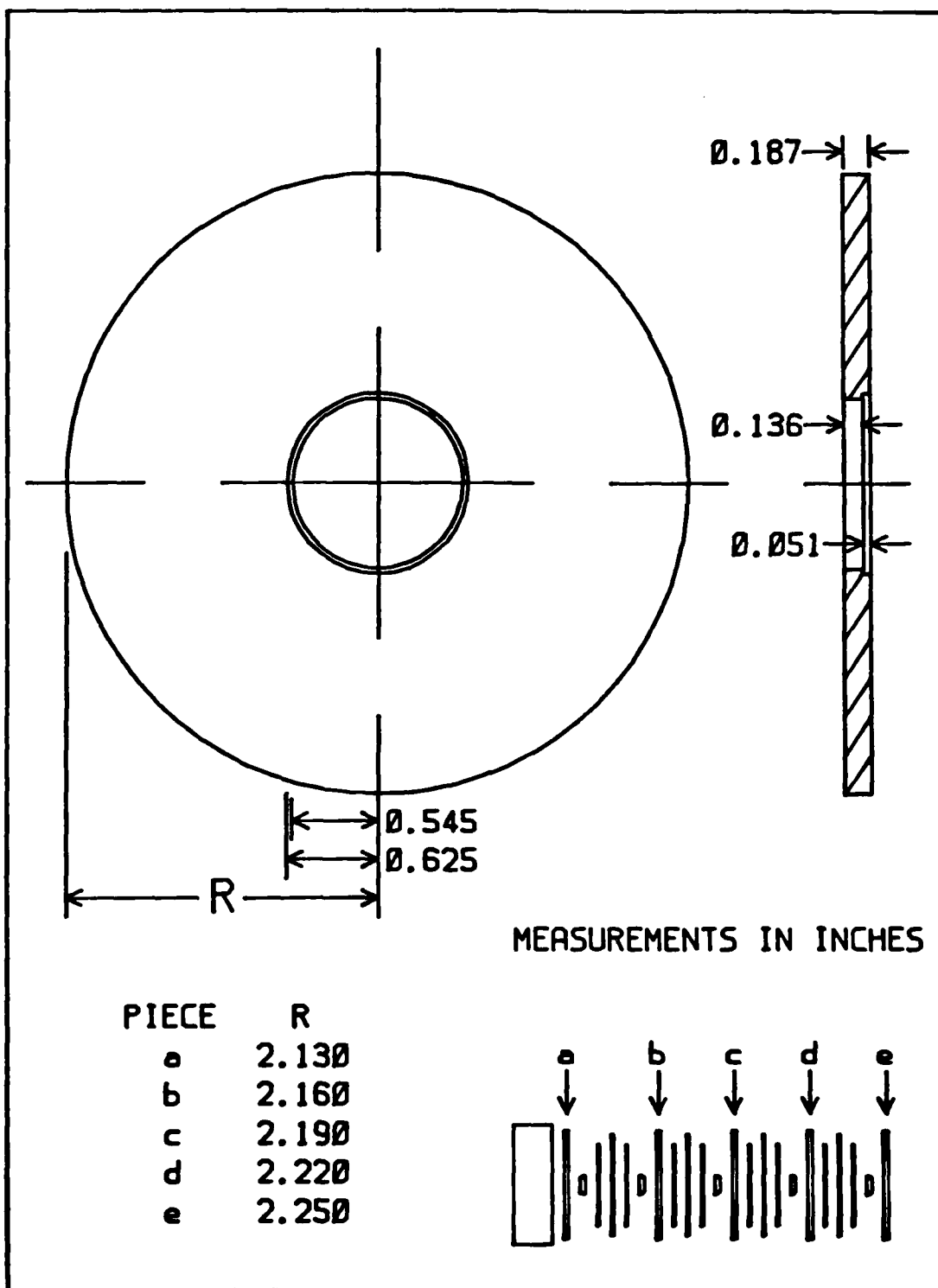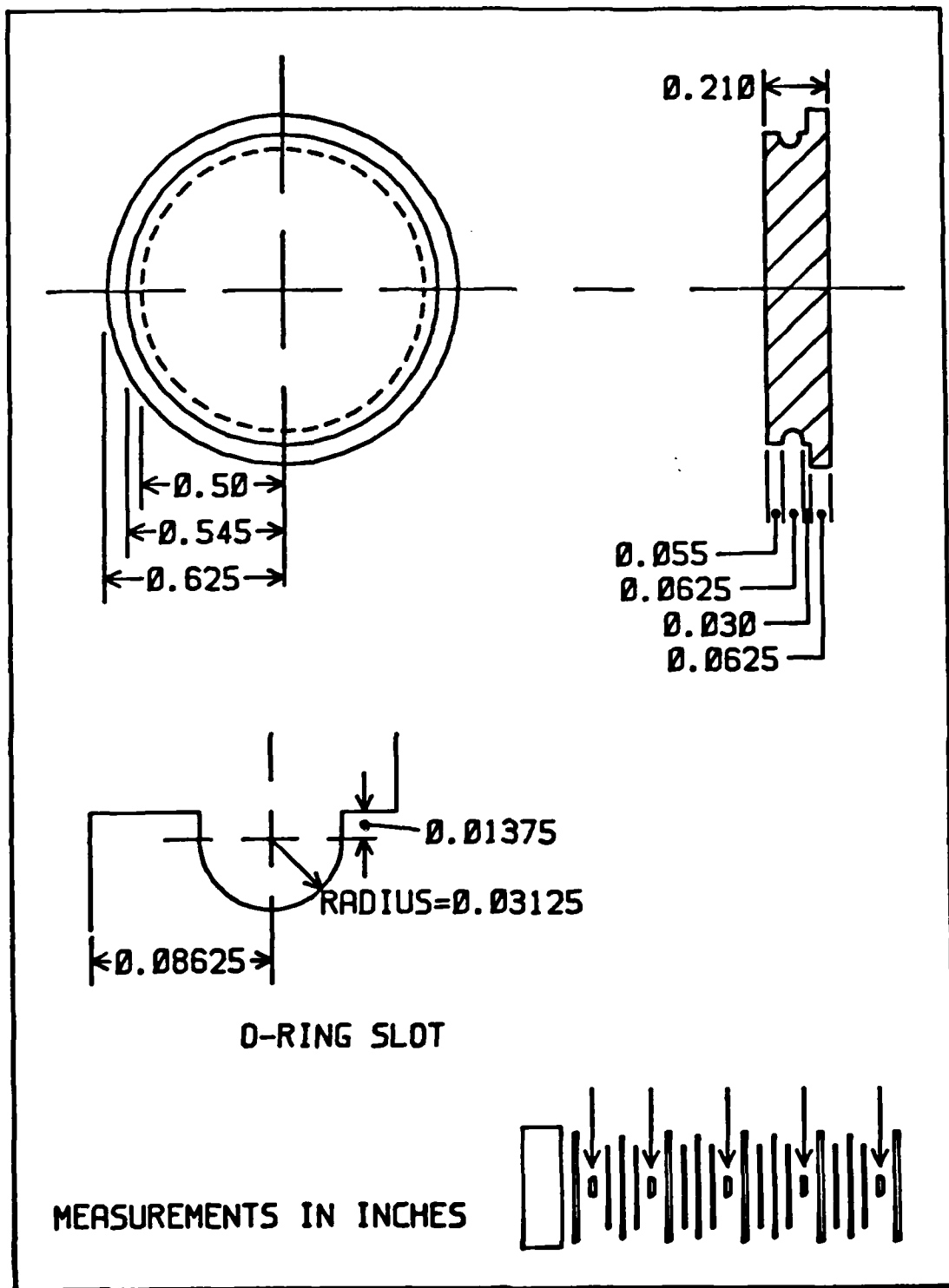
ELECTRICAL INTERCELL CONNECTION (NICKEL SLUG)
FIGURE A-4

0.030

COINED
AREAS

0.015

0.65

1.65

1.69

MEASUREMENTS IN INCHES

N=NICKEL ELECTRODE

C=CADMIUM ELECTRODE

N C N C N C N C
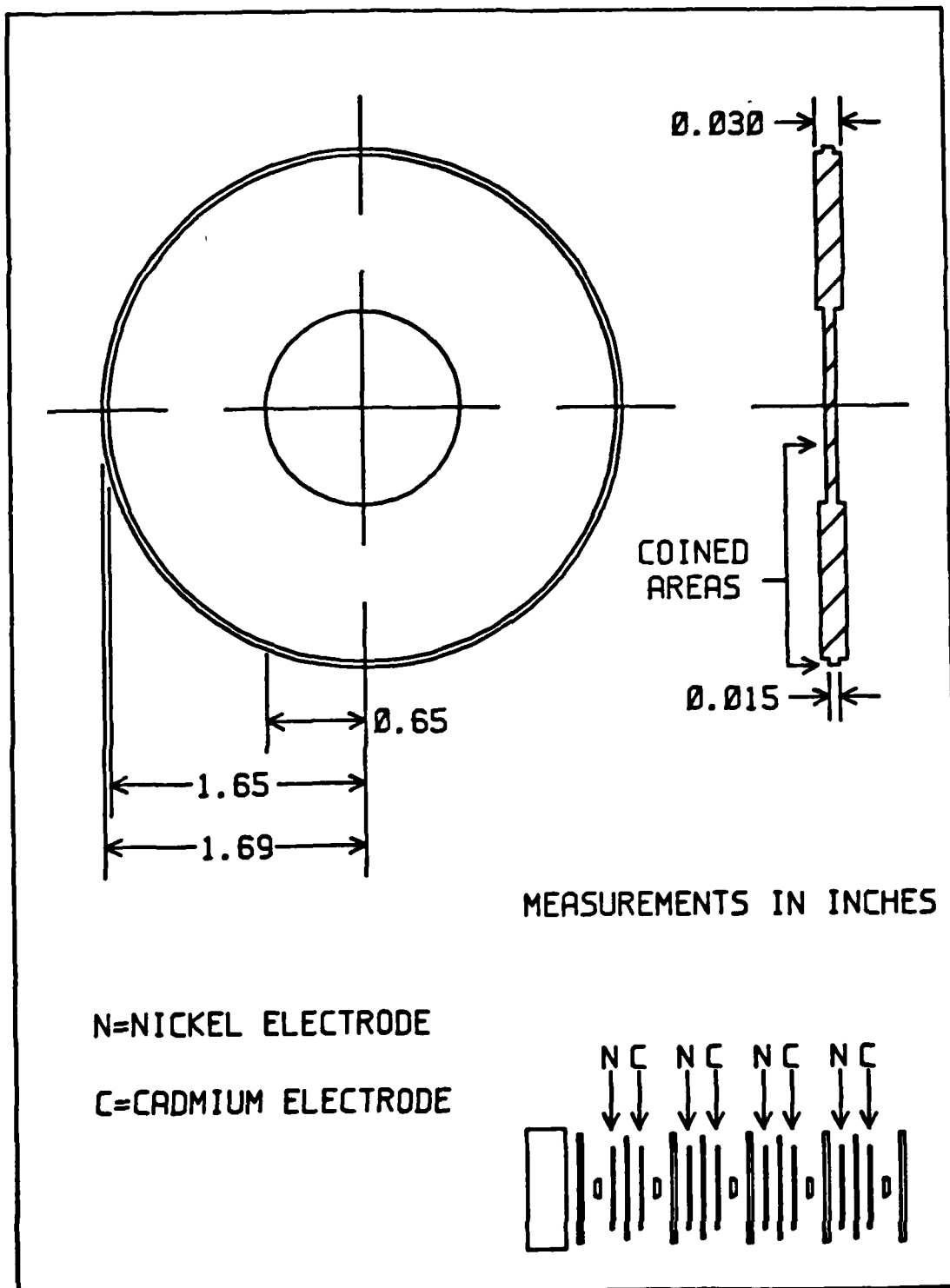
TYPICAL ELECTRODE
FIGURE A-5

Appendix B - Electrode Loading Process

Overview

As pointed out in Chapter 3, both cadmium and nickel electrodes were fabricated in an attempt to improve internal electrode to nickel slug intercell connector welds. Both electrodes were formed on 0.030 inch thick nickel plaques of approximately 80% porosity. Figure B-1 depicts the impregnation apparatus set up. The cadmium electrodes were loaded in accordance with the Fritts, Leonard, and Palanisamy patent [8]. The nickel electrodes were loaded in accordance with the Pickett patent [14], except that the alcohol was replaced by water and 10% cobalt was added to improve the performance of the electrode.

Procedure

The impregnation procedure for both the cadmium and nickel electrodes followed these steps:

1. Four by four inch squares of empty plaque were coined at approximately 7000 pounds per square inch.

2. The plaques were numbered and weighed.

3. The center regions, areas where the welds would be made, were then masked with tape to further inhibit active material loading in this region.

4. Electrochemical loading was completed with either cadmium or nickel.

5. The nickel electrodes were placed in a KOH bath and discharged for 20 minutes followed by a 20 minute

69

charge. This cycle continued for 2 hours and 20 minutes. After the cycling, the electrodes were soaked in distilled water to remove any KOH remaining from the impregnation process.

6. The electrodes were rinsed in distilled water, dried, and then weighed.

7. The increased weight was then used to determine the theoretical capacity of each electrode with cadmium having 0.366 ampere/hours per gram and nickel having 0.289 ampere/hours per gram capacity.

8. Electrodes were grouped by theoretical capacity so that each battery would have approximately the same capacity in each cell.

9. The excess coined area was then cutoff, and the electrode was ready for use in a test battery.

The equipment used is listed in Appendix C.
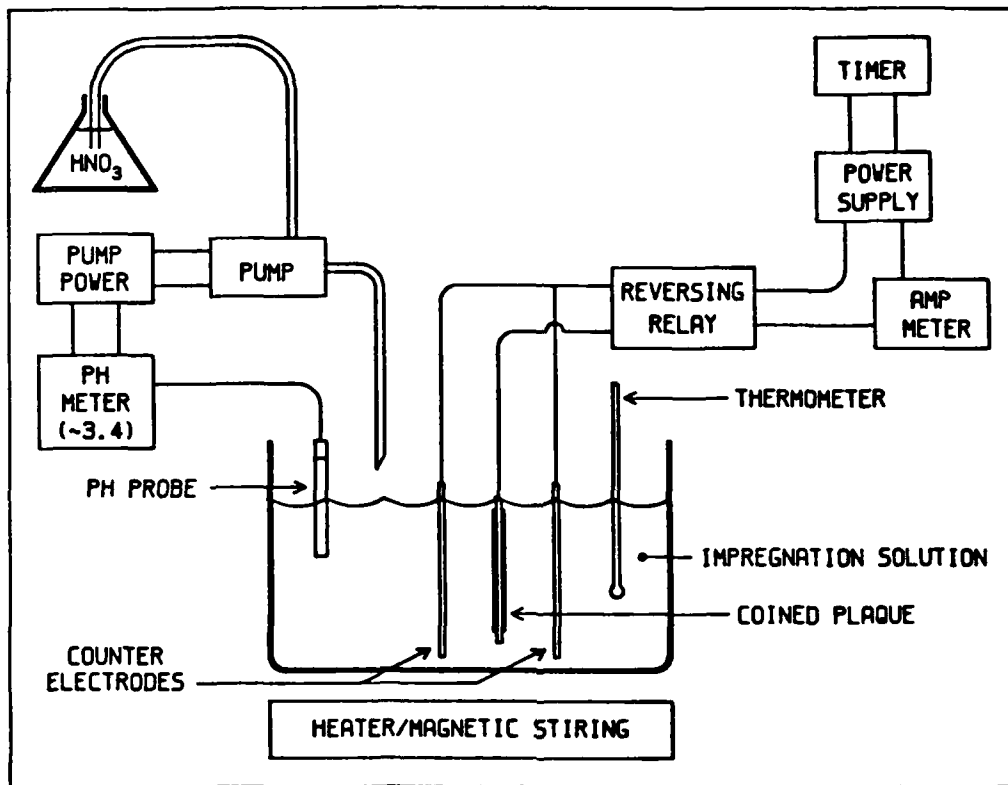
ELECTRODE IMPREGNATION APPARATUS
FIGURE B-1

Appendix C - Test Equipment and Calibration Data

Test Equipment

1   Cole Palmer Pump Model 7013

1   Cole Palmer Pump Power Supply - Master Flux Controller

1   Fisher PH Meter Model 650

1   Fisher Heater/Magnetic Stiring Plate Model 310T

1   Hewlett Packard 4328A Milliohm Meter

1   Hewlett Packard 6263B Power Supply
    20v/10a

2   Hewlett Packard 6012A DC Power Supplies
    0-60v/0-50a, 1000w

1   Hewlett Packard 7418A 8 Channel Recorder with
    5 - 8801A, 1 - 8802A, and 2 - 8803A amplifiers

2   Kiethley 172A Digital Multimeters

1   Lab Fabricated Reversing Relay
    (50 seconds forward, 10 seconds reverse)

1   Lab Fabricated Timer Model 10PCD

1   Power/Mate Corp Lectra-Load II LL300B
    50v, 300a, 1250w

1   Tektronix Oscilloscope
    AN/USM - 425(V)1

1   Transistor Devices Inc. Solid State Load
    Dynaload 50v, 15a, 100w

1   Transistor Devices Inc. Solid State Load
    DLP-50-60-1000 50v, 60a, 1000w

2   Wavetek Voltage Controlled Generators
    VCG Model III

1   Weston Ammeter Model 901

Test Log of Calibration

1 August 1984

> 1200 Battery voltage circuits 1 and 2
>
> Calibrated 0.05v/div, 4 - 6.5v range at:
>
> $$V_B = 4, 5, 6 \text{ v}$$
>
> 1225 Circuit 2 Battery and Power Supply Current
>
> Calibrated 10a/100mv, 5mv/div -- 0.5a/div
>
> $$I_B = 0, -5, -10 \text{ a}$$
>
> $$I_S = 0, 5, 10 \text{ a}$$
>
> 1230 Circuit 2 Load Current
>
> Calibrated 25a/100mv, 4mv/div -- 1a/div at
>
> $$I_L = 0, 5, 10, 15 \text{ a}$$
>
> 1245 Circuit 1 Battery and Power Supply Current
>
> Calibrated 25a/50mv, 2mv/div -- 1a/div at:
>
> $$I_B = 0, -5, \pm10, -15, \pm20, \pm25 \text{ a}$$
>
> $$I_S = 0, 5, 10, 15, 20, 25 \text{ a}$$
>
> 1255 Circuit 1 Load Current
>
> Calibrated 50a/50mv, 1mv/div -- 1a/div at:
>
> $$I_L = 0, 10, 20, 30, 40, 50 \text{ a}$$

Appendix D - Test Data

This appendix contains copies of the data recorded during construction and capacity testing of the test batteries. Tables D-1 and D-2 contain the data obtained from Batteries 3 and 4 during the 10 million cycle test. Figures D-1 through D-8 show the voltage and current waveforms from Battery 7 during the maximum energy density testing. Figures D-9 through D-13 contain electron microscope photographs of nickel and cadmium electrodes both without cycling and after 10 million cycles. Figures D-14 through D-16 are photographs of the batteries during fabrication, an exploded view of a test battery, and an overall view of the test facilities.

BATTERY NUMBER 1

ELECTRODES:

	CELL 1		CELL 2		CELL 3		CELL 4	
	NI	Cd	NI	Cd	NI	Cd	NI	Cd
NUMBER	1	3	2	2	3	1	4	A
WEIGHT	14.7	13.1	14.9	11.3	14.5	10.2	14.8	14.5
THEORETICAL CAPACITY	1.39	2.63	1.39	1.81	1.39	1.49	1.39	2.99

TOTAL ELECTRODE WEIGHT: 108.0 gm / 0.2382 lbs

EQUIVALENT BATTERY WEIGHT: 0.4113 lbs (1.727 x ELECTRODE WEIGHT)

ACTUAL BATTERY WEIGHT: -   gm /   -   lbs (INCLUDING KOH)

CONDITIONING AND CAPACITY CHECKS:

CYCLE	DISCHARGE RATE (amps)	TIME (minutes)	CAPACITY (amp/hours)	TEST CIRCUIT
1	1.0	7	0.11	1
2	0.3	76	0.38	1

75

BATTERY NUMBER   2

ELECTRODES:

	CELL 1		CELL 2		CELL 3		CELL 4	
	NI	Cd	NI	Cd	NI	Cd	NI	Cd
NUMBER	5	14	6	15	7	16	9	18
WEIGHT	15.0	11.8	14.7	13.2	15.2	13.2	14.9	13.1
THEORETICAL CAPACITY	1.39	2.28	1.39	2.97	1.39	3.10	1.39	2.69

TOTAL ELECTRODE WEIGHT: 111.1 gm / 0.2451 lbs

EQUIVALENT BATTERY WEIGHT: 0.4231 lbs (1.727 x ELECTRODE WEIGHT)

ACTUAL BATTERY WEIGHT: -   gm /   -   lbs (INCLUDING KOH)

CONDITIONING AND CAPACITY CHECKS:

CYCLE	DISCHARGE RATE (amps)	TIME (minutes)	CAPACITY (amp/hours)	TEST CIRCUIT
1	1.0	35	0.58	2
2	0.6	87	0.87	2
3	0.8	2	-	2
4	0.7	55	0.64	2
5	1.0	39	0.66	1

BATTERY NUMBER 3

ELECTRODES:

	CELL 1		CELL 2		CELL 3		CELL 4	
	NI	Cd	NI	Cd	NI	Cd	NI	Cd
NUMBER	11	21	12	24	14	25	13	45
WEIGHT	15.7	13.9	15.7	14.0	15.5	15.3	15.9	13.9
THEORETICAL CAPACITY	1.39	2.91	1.39	2.92	1.39	2.95	1.39	2.96

TOTAL ELECTRODE WEIGHT: 111.9 gm / 0.2468 lbs

EQUIVALENT BATTERY WEIGHT: 0.4262 lbs (1.727 x ELECTRODE WEIGHT)

ACTUAL BATTERY WEIGHT: 936.8 gm / 2.067 lbs (INCLUDING KOH)

CONDITIONING AND CAPACITY CHECKS:

CYCLE	DISCHARGE RATE (amps)	TIME (minutes)	CAPACITY (amp/hours)	TEST CIRCUIT
1	1.0	60	1.00	1
2	1.0	35	0.58	1
3	1.0	63	1.05	1
4	1.0	62	1.03	1
5	1.5	40	1.00	1
6	1.0	55	0.92	2
7	1.0	59	0.98	2
8	1.0	48	0.80	2
9	1.0	48	0.80	2
10	1.0	45	0.75	2

BATTERY NUMBER   4

ELECTRODES:

	CELL 1		CELL 2		CELL 3		CELL 4	
	NI	Cd	NI	Cd	NI	Cd	NI	Cd
NUMBER	15	42	16	44	17	46	19	48
WEIGHT	15.5	13.4	15.0	13.6	15.5	14.0	15.3	13.6
THEORETICAL CAPACITY	1.39	2.67	1.39	2.80	1.39	2.70	1.39	2.68

TOTAL ELECTRODE WEIGHT: 115.9 gm / 0.2557 lbs

EQUIVALENT BATTERY WEIGHT: 0.4415 lbs (1.727 × ELECTRODE WEIGHT)

ACTUAL BATTERY WEIGHT: 924.7 gm / 2.040 lbs (INCLUDING KOH)

CONDITIONING AND CAPACITY CHECKS:

CYCLE	DISCHARGE RATE (amps)	TIME (minutes)	CAPACITY (amp/hours)	TEST CIRCUIT
1	1.0	24	0.40	2
2	1.0	50	0.83	2
3	1.0	50	0.83	2
4	1.0	30	0.50	2
5	1.0	57	0.95	2
6	1.0	56	0.93	2
7	1.5	36	0.90	2
8	1.0	53	0.88	1
9	1.0	56	0.93	1
10	1.0	45	0.75	2

BATTERY NUMBER   5

ELECTRODES:

	CELL 1		CELL 2		CELL 3		CELL 4	
	NI	Cd	NI	Cd	NI	Cd	NI	Cd
NUMBER	21	37	20	49	23	38	22	55
WEIGHT	15.6	12.5	15.9	12.2	15.5	12.9	15.2	12.5
THEORETICAL CAPACITY	1.39	2.23	1.39	2.24	1.39	2.27	1.39	2.28

TOTAL ELECTRODE WEIGHT: 112.3 gm / 0.2478 lbs

EQUIVALENT BATTERY WEIGHT: 0.4278 lbs (1.727 x ELECTRODE WEIGHT)

ACTUAL BATTERY WEIGHT: 931.0 gm / 2.054 lbs (INCLUDING KOH)

CONDITIONING AND CAPACITY CHECKS:

CYCLE	DISCHARGE RATE (amps)	TIME (minutes)	CAPACITY (amp/hours)	TEST CIRCUIT
1	1.0	28	0.47	1
2	1.0	38	0.63	1
3	1.0	38	0.63	1
4	1.0	37	0.62	1
5	1.0	39	0.66	1

BATTERY NUMBER   6

ELECTRODES:

	CELL 1		CELL 2		CELL 3		CELL 4	
	NI	Cd	NI	Cd	NI	Cd	NI	Cd
NUMBER	24	53	25	36	26	50	27	29
WEIGHT	15.2	13.3	15.8	13.5	15.5	13.7	15.7	13.3
THEORETICAL CAPACITY	1.39	2.73	1.39	2.77	1.39	2.81	1.39	2.84

TOTAL ELECTRODE WEIGHT: 116.0 gm / 0.2559 lbs
EQUIVALENT BATTERY WEIGHT: 0.4419 lbs (1.727 x ELECTRODE WEIGHT)
ACTUAL BATTERY WEIGHT: 924.6 gm / 2.080 lbs (INCLUDING KOH)

CONDITIONING AND CAPACITY CHECKS:

CYCLE	DISCHARGE RATE (amps)	TIME (minutes)	CAPACITY (amp/hours)	TEST CIRCUIT
1	1.0	0	0.00	2

BATTERY NUMBER 7

ELECTRODES:

	CELL 1		CELL 2		CELL 3		CELL 4	
	NI	Cd	NI	Cd	NI	Cd	NI	Cd
NUMBER	100	23	97	22	98	47	92	33
WEIGHT	12.0	14.2	12.0	14.5	12.0	15.1	12.3	14.5
THEORETICAL CAPACITY	1.65	3.22	1.66	3.18	1.68	3.19	1.69	3.17

TOTAL ELECTRODE WEIGHT: 106.6 gm / 0.2351 lbs

EQUIVALENT BATTERY WEIGHT: 0.4061 lbs (1.727 x ELECTRODE WEIGHT)

ACTUAL BATTERY WEIGHT: 918.9 gm / 2.027 lbs (INCLUDING KOH)

CONDITIONING AND CAPACITY CHECKS:

CYCLE	DISCHARGE RATE (amps)	TIME (minutes)	CAPACITY (amp/hours)	TEST CIRCUIT
1	1.0	44	0.73	1
2	1.0	47	0.78	1
3	1.0	45	0.75	1
4	1.0	39	0.65	1
5	1.0	40	0.67	1
6	1.0	40	0.67	1
7	1.0	20	0.33	1
8	1.0	39	0.65	1
9	1.0	40	0.67	1
51 ∎	1.0	60	1.00	1
52 ∎	1.0	61	1.02	1

∎ AN AUTOMATIC SERIES OF DEEP DISCHARGE AND CHARGE CYCLES WAS COMPLETED BEFORE THESE MEASUREMENTS WERE TAKEN.

81

TABLE D-1
10^7 CYCLE TEST, BATTERY 3 (20 AUG TO 13 SEP 1984)

| CYCLES (MILLIONS)	AVERAGE VOLTAGE (VOLTS)	ENERGY DENSITY (JOULES/POUND)	EFFICIENCY (%)	CAPACITANCE (FARADS)
0.27	5.18	7.20	88.6	2.6
0.39	*	7.20	84.6	2.7
0.83	5.15	7.18	87.3	2.5
1.23	5.18	7.0	84.0	2.0
1.69	5.02	7.0	82.7	0.84
2.07	5.21	7.2	81.9	0.72
2.29	5.18	7.1	86.4	0.74
2.67	5.17	7.1	82.8	0.85
2.98	5.18	7.1	82.3	0.75
3.42	5.18	7.2	84.9	0.75
3.86	5.23	7.2	82.7	0.77
4.29	5.25	7.09	81.8	0.63
4.72	5.18	6.99	81.3	0.71
4.86	4.98	7.46	84.5	0.71 **
5.19	5.14	7.20	82.7	3.60
5.61	5.12	7.55	87.6	3.19
6.06	5.12	7.54	87.6	2.68
6.48	5.30	7.63	85.6	1.89
6.83	5.28	7.24	83.6	2.20
7.26	5.18	7.83	84.5	2.38
7.78	5.11	7.25	83.1	3.88
8.10	5.27	7.23	84.5	2.48
8.67	5.63	7.83	88.4	1.18
8.99	5.19	7.18	84.3	2.25
9.43	5.14	7.18	85.3	2.88
9.86	5.16	7.17	85.6	2.06
10.22	*	7.41	88.7	1.56

* NO VOLTAGE READING TAKEN.

** THE BATTERY WAS REMOVED FROM THE TEST CIRCUIT, CAPACITY CHECKED, CHARGED TO 60% OF MEASURED CAPACITY AND RETURNED TO THE TEST CIRCUIT.

TABLE D-2
10^7 CYCLE TEST, BATTERY 4 (20 AUG TO 12 SEP 1984)

CYCLES (MILLIONS)	AVERAGE VOLTAGE (VOLTS)	ENERGY DENSITY (JOULES/POUND)	EFFICIENCY (%)	CAPACITANCE (FARADS)
0.27	5.12	12.95	85.1	3.2
0.39	*	13.6	84.6	3.2
0.83	5.12	13.7	82.5	2.6
1.23	5.19	13.6	77.2	1.7
1.69	5.08	13.8	82.9	1.5
2.07	5.22	14.3	83.7	1.4
2.29	5.16	14.1	83.3	1.5
2.67	5.17	14.1	83.0	1.6
2.98	5.32	14.65	85.2	2.4
3.42	5.33	14.65	85.6	2.3
3.86	5.36	14.7	85.5	2.1
4.29	5.24	14.47	84.2	2.1
4.72	5.24	14.63	88.0	2.3
5.20	5.20	14.20	87.0	3.0
5.62	5.10	13.92	85.6	3.0
6.03	5.30	14.75	85.4	2.2
6.55	5.31	14.6	85.2	2.4
6.89	5.32	14.7	86.0	2.2
7.32	5.21	13.9	82.3	2.42
7.75	5.30	14.3	82.6	2.0
8.19	5.20	14.6	82.1	2.50
8.63	5.23	14.3	85.2	2.43
9.06	5.32	14.0	88.5	2.10
9.48	5.27	14.32	87.0	2.46
9.91	5.25	14.1	84.3	2.40
10.00	5.26	14.7	86.6	2.17

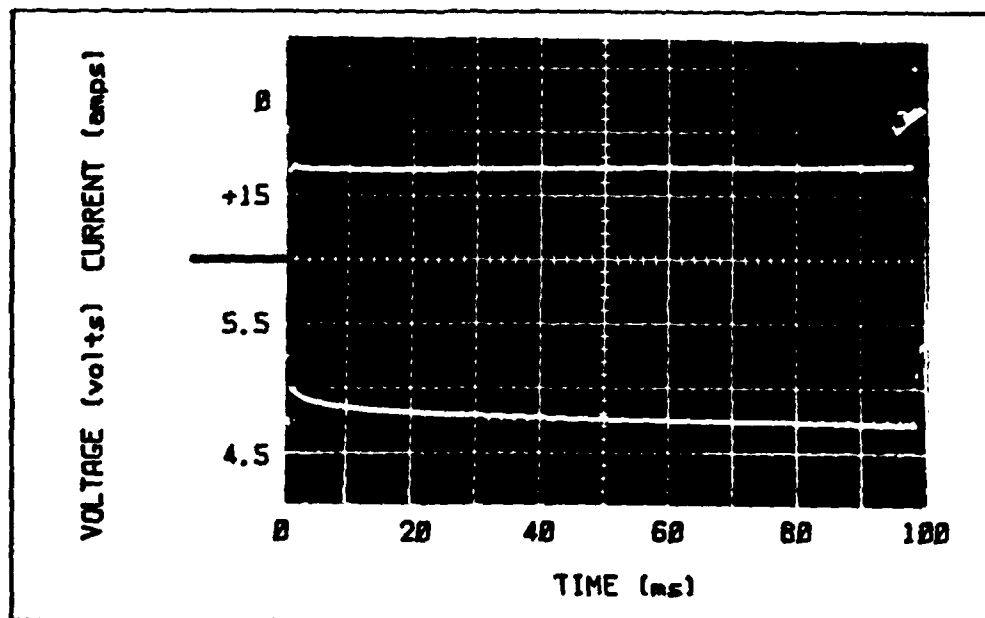* NO VOLTAGE READING TAKEN.
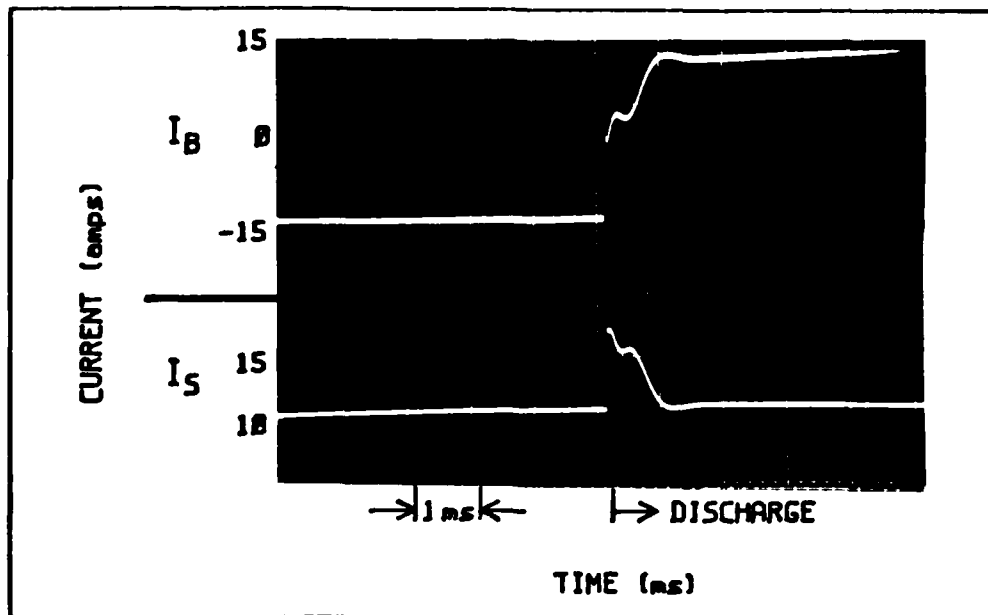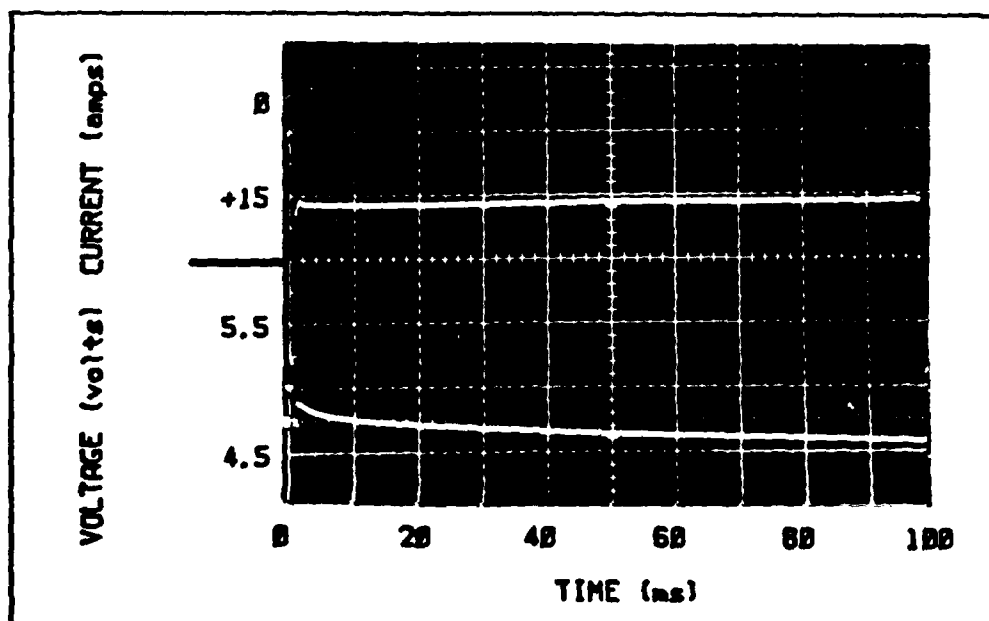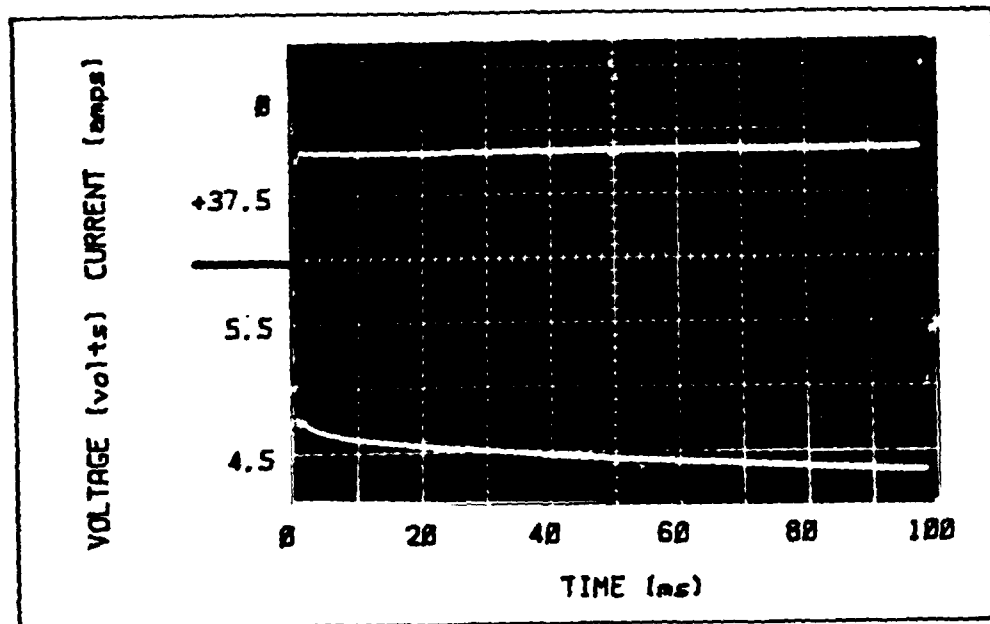
TYPICAL POWER SUPPLY CURRENT WAVEFORM
FIGURE D-1
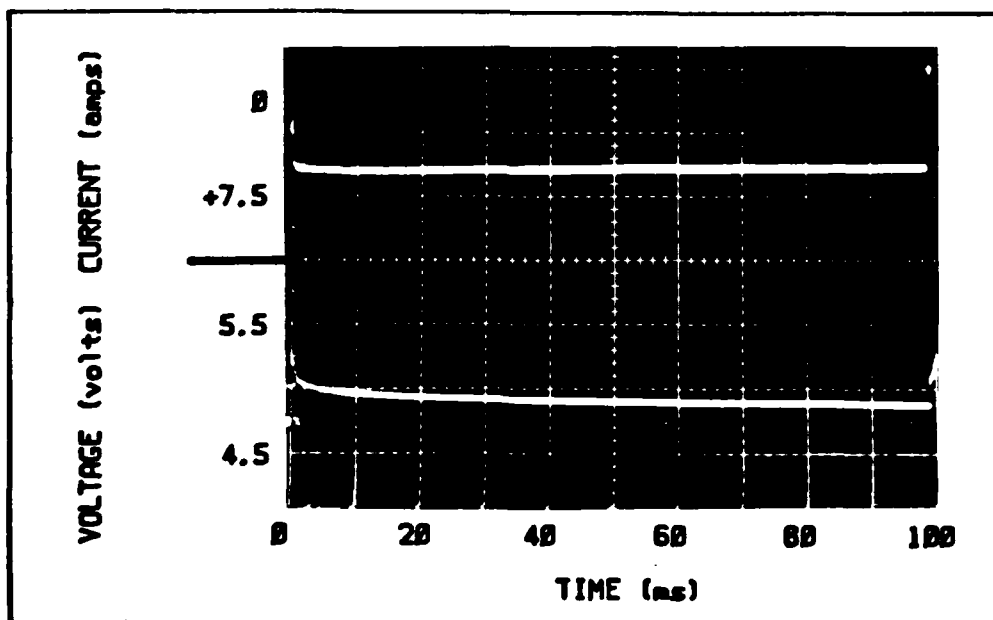
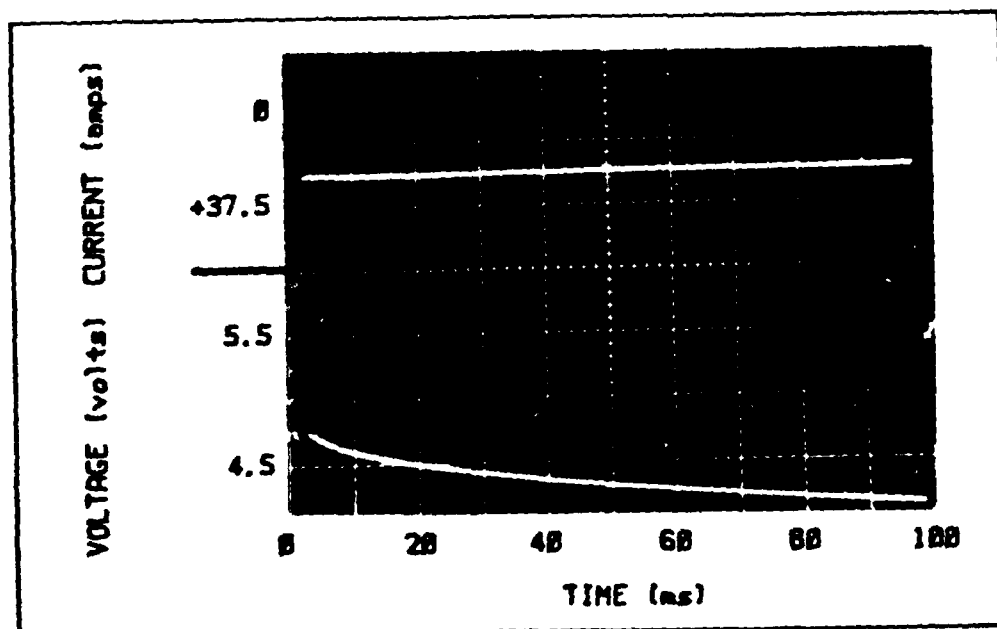BATTERY 7 DISCHARGE VOLTAGE AND CURRENT (I_B=5amps)
FIGURE D-2

BATTERY 7 DISCHARGE VOLTAGE AND CURRENT (I_B=10 amps)
FIGURE D-3

BATTERY 7 DISCHARGE VOLTAGE AND CURRENT (I_B=15amps)
FIGURE D-4

85

BATTERY 7 DISCHARGE VOLTAGE AND CURRENT (I_B=20 amps)
FIGURE D-5

BATTERY 7 DISCHARGE VOLTAGE AND CURRENT (I_B=25amps)
FIGURE D-6

B6

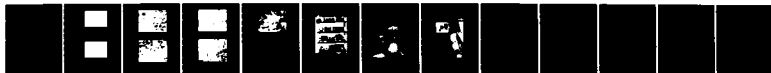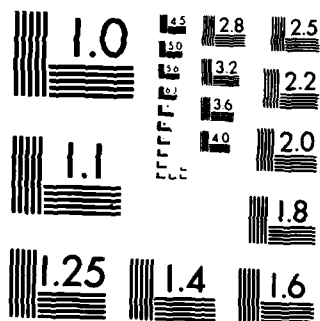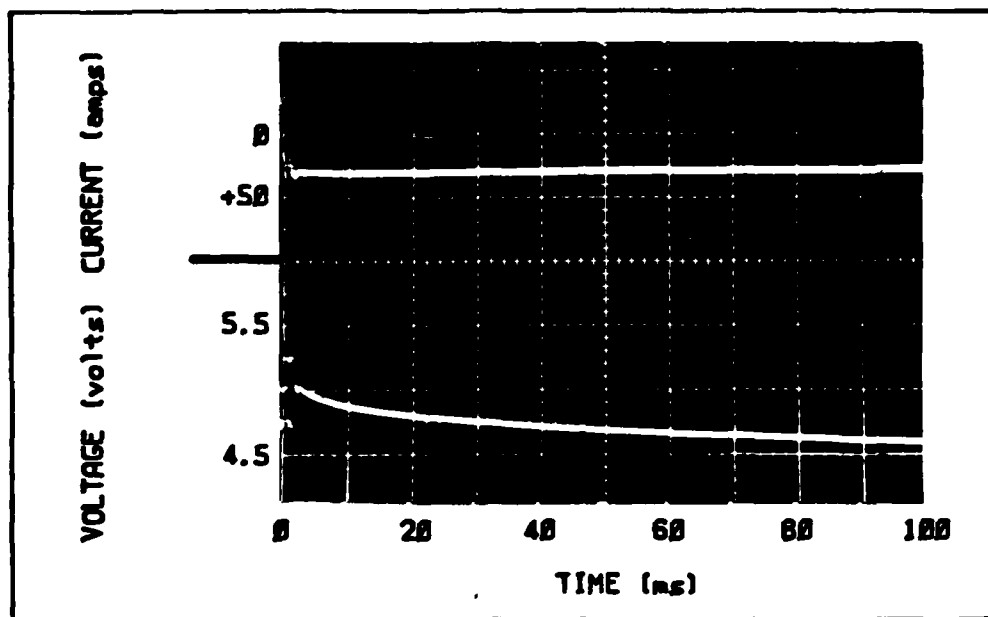MICROCOPY RESOLUTION TEST CHART

NATIONAL BUREAU OF STANDARDS 1963 A
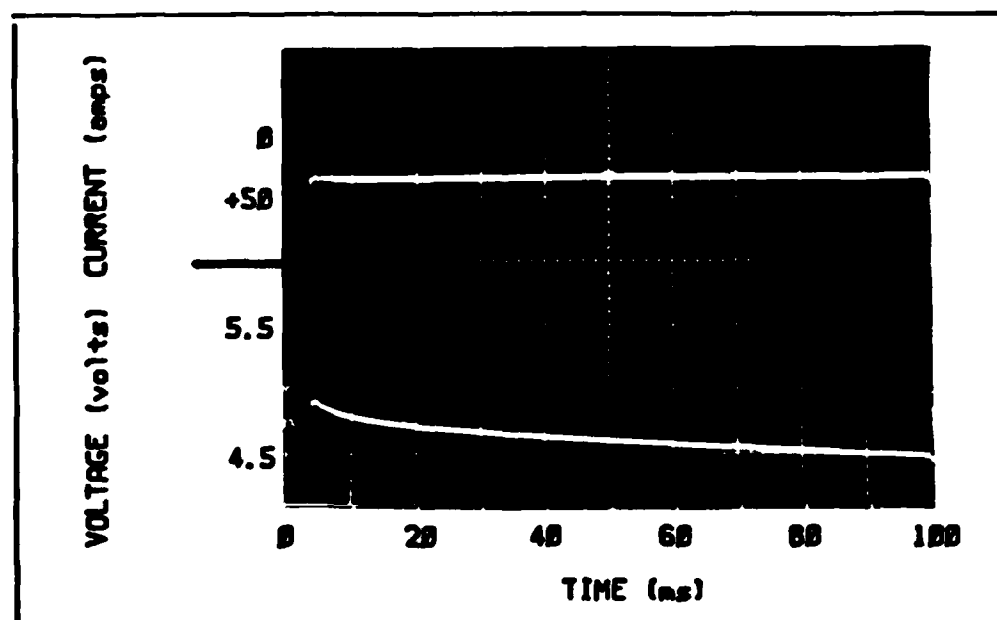
BATTERY 7 DISCHARGE VOLTAGE AND CURRENT (I_B=30 amps)
FIGURE D-7

BATTERY 7 DISCHARGE VOLTAGE AND CURRENT (I_B=35amps)
FIGURE D-8

87

UNCYCLED NICKEL ELECTRODE (75X, 375X)
FIGURE D-9
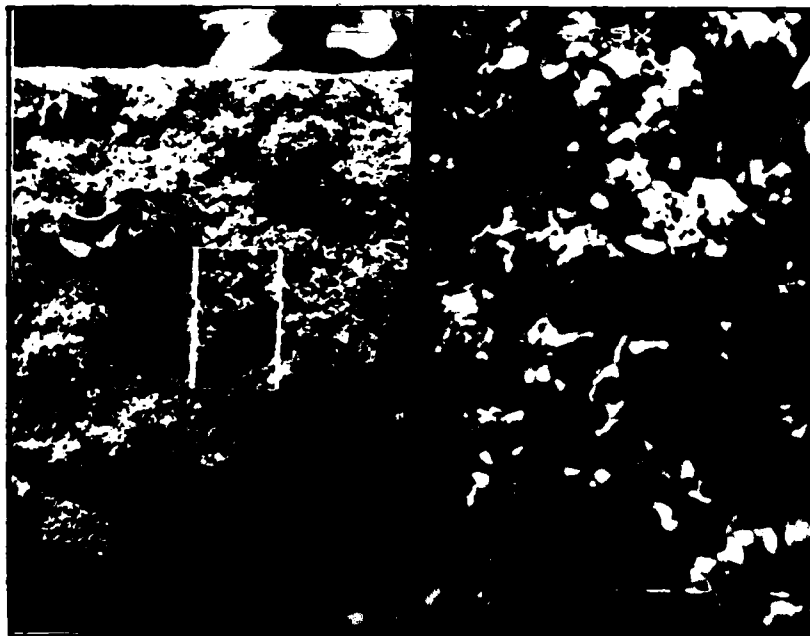
CYCLED NICKEL ELECTRODE (75X, 375X)
FIGURE D-10

88

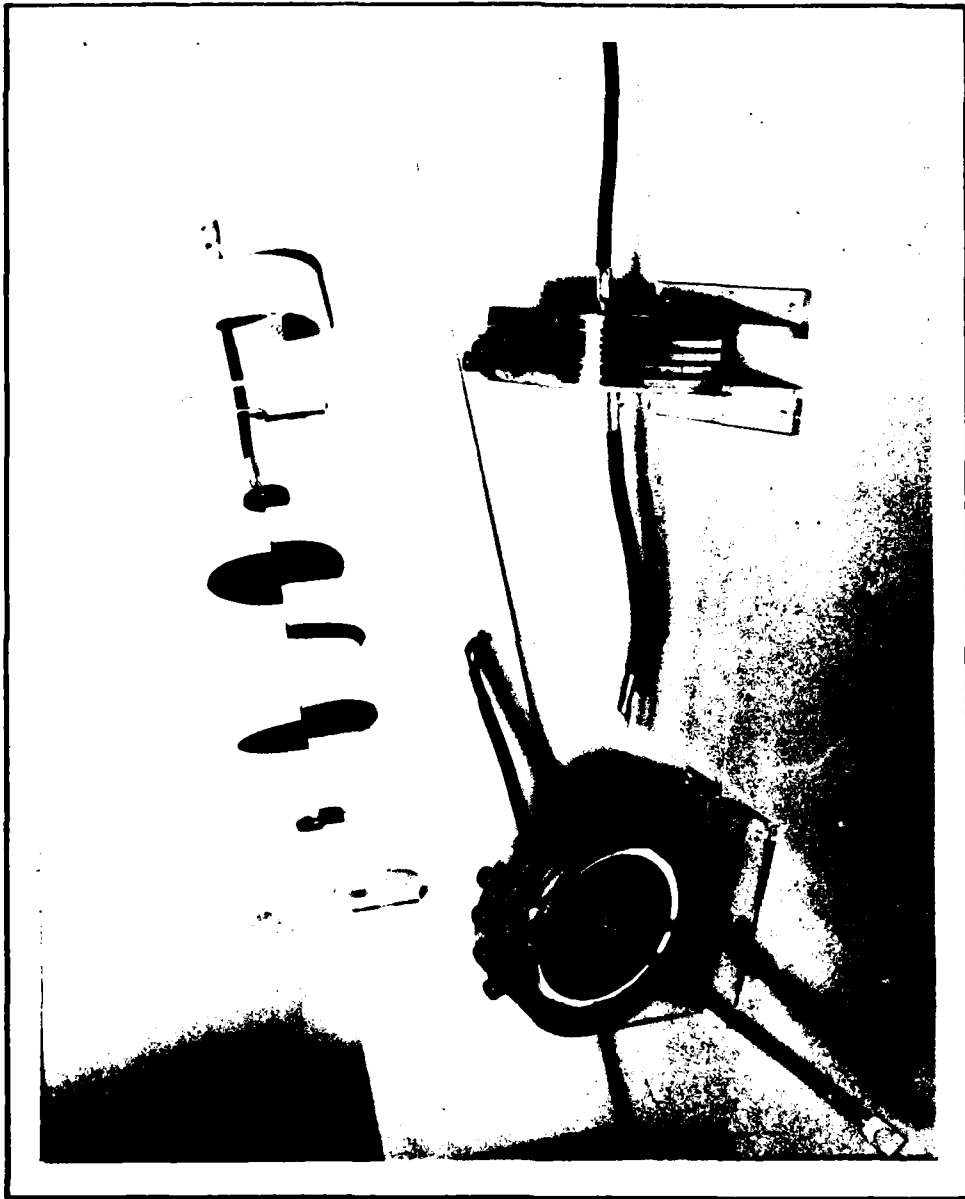UNCYCLED CADMIUM ELECTRODE (75X, 375X)
FIGURE D-11

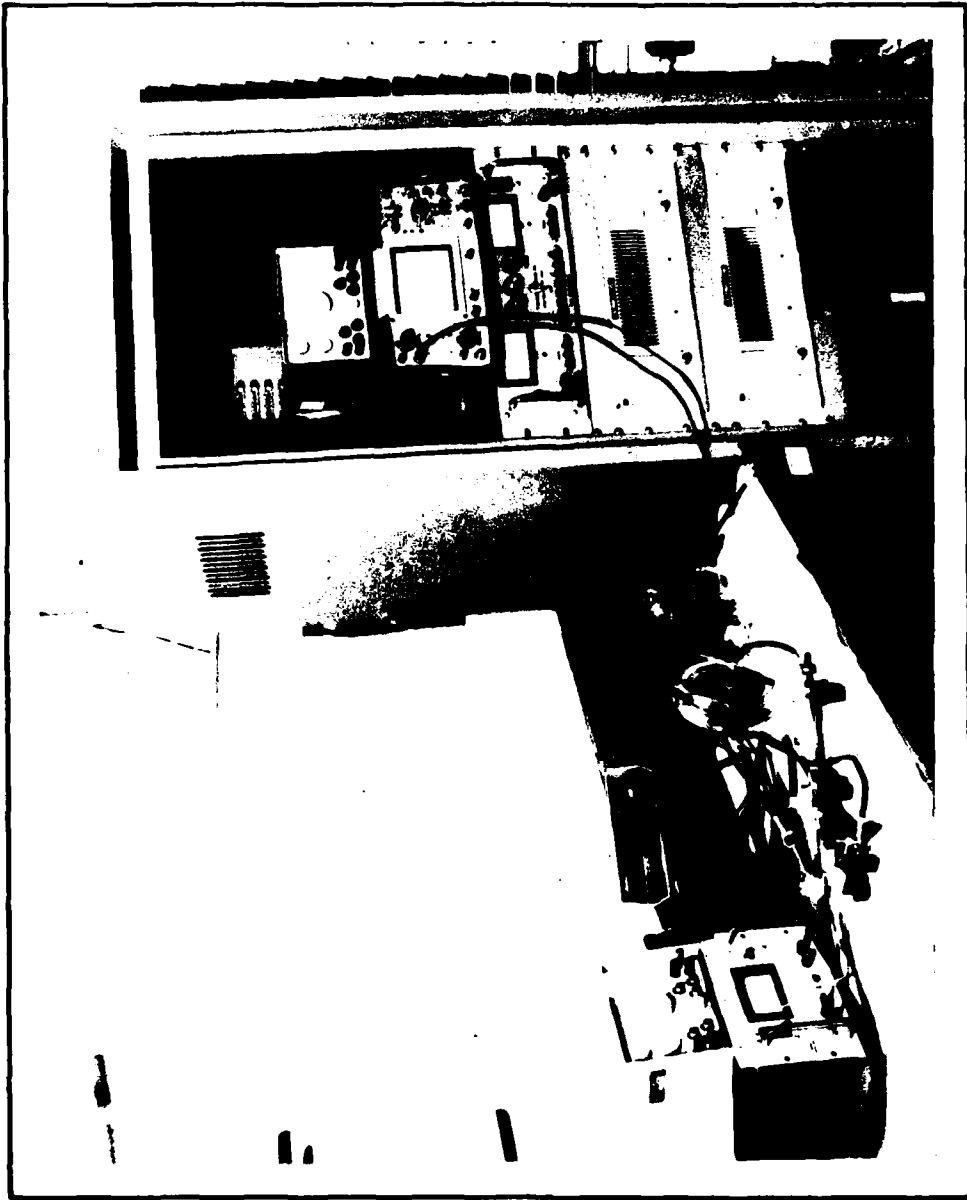CYCLED CADMIUM ELECTRODE (75X, 375X)
FIGURE D-12

CYCLED CADMIUM ELECTRODE (3700X)
FIGURE D-13

BATTERY PARTS IN VARIOUS STAGES OF ASSEMBLY
FIGURE D-14

EXPLODED VIEW OF THE TEST BATTERY
FIGURE D-15

VIEW OF TEST FACILITIES
FIGURE D-16

Bibliography

1. Amile, R.F., J.B. Ockerman, and P. Ruetshci. "Absorption of Hydrogen and Oxygen on Electrode Surfaces". Journal of the Electrochemical Society, 108: 377, 1961.

2. Bauer, P. Batteries for Space Power Systems. Washington D.C.: NASA, 1968. (NASA SP172).

3. Bishop, W.S. "Batteries and Fuel Cells for Pulsed Power Applications." Pulsed Power Lecture Series (15). Plasma and Switching Laboratory, Department of Electrical Engineering, Texas Tech University, Lubbock, Texas, 1981.

4. -----. Investigation of High Discharge Rate Characteristics of Batteries for Pulsed Power Applications. Proposed AFIT Thesis Topic Paper. Aero Propulsion Laboratory, AF Wright Aeronautical Laboratories, Wright-Patterson AFB, Ohio, 1984.

5. ----- and D.C. Stumpff. Evaluation of Nickel-Cadmium Batteries for Long Life, High Repetition Rate Cycling Applications. Unpublished test report. Aero Propulsion Laboratory, AF Wright Aeronautical Laboratories, Wright-Patterson AFB, Ohio, December 1982.

6. Clifford, J.E. Study of Bipolar Batteries. BATTELLE, Columbus Laboratories, Columbus, Ohio, June 1984. (SAND84-7108).

7. Fritts, D.H. Project Engineer, Aero Propulsion Laboratory, AF Wright Aeronautical Laboratories (interview). Wright-Patterson AFB, Ohio, 31 January 1984.

8. -----, et. al. Methods of Fabricating Cadmium Electrodes. U.S. Patent 4,242,179, December 30, 1980.

9. General Electric. Nickel-Cadmium Battery Application Engineering Handbook. Gainesville, Florida, General Electric Company, 1975.

10. Gilmour, A.S. Jr. Investigation of Power Processing Technology for Spacecraft Applications. Technical report AFWAL-TR-82-2054. Aero Propulsion Laboratory, AF Wright Aeronautical Laboratories, Air Force Systems Command, Wright-Patterson AFB, Ohio, June 1982 (AD-A119 644/3).

11. Goddard Space Flight Center. Accelerated Test Plan for Nickel Cadmium Spacecraft Batteries. Greenbelt, Maryland, October 1973. (NASA-TM-X-70524).

12. Milner, P.C. and U. B. Thomas. "The Nickel-Cadmium Cell." Advances in Electrochemistry and Electrochemical Engineering, Vol 5. 1-86. Edited by C.W. Tobias. New York: Interscience Publishers, 1967.

13. Naval Weapons Support Center. 19th Annual Report of Cyclic Life Testing. Crane, Indiana, 1983. (WQEC/C 83-1).

14. Pickett, D.F.   U.S. Patent 3,827,911. 1974.

15. Stevens, N.J.   "Summary of High Voltage Solar Array Interactions with Space Plasma Environments." USAF/ NASA Spacecraft Environmental Interactions Technology Conference Abstracts 41. US Air Force Academy, Colorado, 4-6 October 1983.

16. The McGraw-Hill Encyclopedia of Space. New York: McGraw-Hill Book Company, 1968.

Vita

Major Michael B. Cimino was born on 23 June 1947 in Palo Alto, California. He graduated from high school in Los Altos, California in 1966 and received his Bachelor of Science degree from the University of Idaho in 1971. He received his commission in the United States Air Force through ROTC. He was employed by the Bechtel Corporation in Wyoming until being called to active duty in 1972. He completed pilot training and received his wings the following year. He was assigned to the 56th Special Operations Wing flying EC-47's out of Nakhom Phanom, Thailand. Upon completion of his SEA tour he was assigned to the 410th Bombardment Wing flying KC-135's out of K.I. Sawyer AFB, Michigan. In 1979 he was reassigned to Moody AFB, Georgia where he flew the F-4E for the 347th Tactical Fighter Wing until entering the School of Engineering, Air Force Institute of Technology in June 1983.

Permanent Address: 3 Thunderbird Lane

Pinehurst, North Carolina 28374

Vita

Captain Gregory M. Gearing was born on December 23, 1954 in Inglewood, California. He graduated from Don Bosco Technical Institute, Rosemead, California in 1972. He received his Bachelor of Science degree from the University of California at Berkeley in 1976. He received his commission in the United States Air Force through ROTC the same year. Until being called to active duty in 1977 he was employed as a project engineer by Texas Instruments. He completed pilot training and received his wings the following year. He was assigned to the 42nd Bombardment Wing, Loring AFB, Maine flying B-52G's. He entered the School of Engineering, Air Force Institute of Technology in June 1983. The following year he was nominated to become a member of Tau Beta Pi and Eta Kappa Nu.

> Permanent Address: 220 N. Highland Place
> Monrovia, California 91016

REPORT DOCUMENTATION PAGE

1a. REPORT SECURITY CLASSIFICATION UNCLASSIFIED		1b. RESTRICTIVE MARKINGS N/A			
2a. SECURITY CLASSIFICATION AUTHORITY		3. DISTRIBUTION/AVAILABILITY OF REPORT Approved for Public Release Distribution Unlimited			
2b. DECLASSIFICATION/DOWNGRADING SCHEDULE N/A					
4. PERFORMING ORGANIZATION REPORT NUMBER(S) AFIT/GE/ENG/84D-18		5. MONITORING ORGANIZATION REPORT NUMBER(S)			
6a. NAME OF PERFORMING ORGANIZATION School of Engineering	6b. OFFICE SYMBOL (If applicable) AFIT/EN	7a. NAME OF MONITORING ORGANIZATION N/A			
6c. ADDRESS (City, State and ZIP Code) Air Force Institute of Technology Wright-Patterson AFB, OH 45433		7b. ADDRESS (City, State and ZIP Code) N/A			
8a. NAME OF FUNDING/SPONSORING ORGANIZATION Aero Propulsion Laboratory	8b. OFFICE SYMBOL (If applicable) POOC-1	9. PROCUREMENT INSTRUMENT IDENTIFICATION NUMBER			
8c. ADDRESS (City, State and ZIP Code) Air Force Wright Aeronautical Laboratories Wright-Patterson AFB, OH 45433		10. SOURCE OF FUNDING NOS			
11. TITLE (Include Security Classification) See Item 19.*		PROGRAM ELEMENT NO. 62203F	PROJECT NO. 3145	TASK NO. 22	WORK UNIT NO. 33
12. PERSONAL AUTHOR(S) Michael B. Cimino, Major, USAF			Gregory M. Gearing, Captain, USAF		
13a. TYPE OF REPORT MS Thesis	13b. TIME COVERED FROM _____ TO _____	14. DATE OF REPORT (Yr., Mo., Day) 1984 December		15. PAGE COUNT 108	
16. SUPPLEMENTARY NOTATION					

17.	COSATI CODES		18. SUBJECT TERMS (Continue on reverse if necessary and identify by block number)
FIELD	GROUP	SUB. GR.	Nickel Cadmium Battery, Bi-polar Nickel Cadmium Battery, Capacitive Filter, Life Cycle Testing
10	03		
09	01		

19. ABSTRACT (Continue on reverse if necessary and identify by block number)

<u>Item 11. TITLE:</u>   Investigation of Pseudo Bi-polar Nickel Cadmium Batteries as Filter Elements for Pulsed Power Loads (Unclassified)

Approved for public release: IAW AFR 190-17.

[signature]   *15 Feb 85*
Dean for Research and Professional Development
Air Force Institute of Technology (ATC)
Wright-Patterson AFB OH 45433

20. DISTRIBUTION/AVAILABILITY OF ABSTRACT UNCLASSIFIED/UNLIMITED ☒ SAME AS RPT. ☐ DTIC USERS ☐	21. ABSTRACT SECURITY CLASSIFICATION UNCLASSIFIED	
22a. NAME OF RESPONSIBLE INDIVIDUAL ANDREW J. TERZUOLI JR., GM-13	22b. TELEPHONE NUMBER (Include Area Code) (513) 255-2024	22c. OFFICE SYMBOL AFIT/EN

DD FORM 1473, 83 APR   EDITION OF 1 JAN 73 IS OBSOLETE.

ABSTRACT

This investigation consisted of several tests of specially fabricated nickel-cadmium batteries having circular disk type electrodes. These batteries were evaluated as filter elements between a constant current power supply and a five hertz pulsed load demanding approximately twice the power supply current during the load on portion of the cycle. Short tests lasting 10^4 cycles were conducted at up to a 21 C rate and an equivalent energy density of over 40 Joules per pound. In addition, two batteries were subjected to 10^7 charge/discharge cycles, one at a 6.5 C rate and the other at a 13 C rate. Assuming an electrode to battery weight ratio of 0.5, these tests represent an energy density of about 7 and 14 Joules per pound respectively. Energy density, efficiency, capacitance, average voltage, and available capacity were tracked during these tests. After 10^7 cycles, capacity degradation was negligible for one battery and about 20% for another. Cadmium electrode failure may be the lifetime limiting factor at extremely low depth of discharge cycling. The output was examined and a simple equivalent circuit is proposed.

END

FILMED

5-85

DTIC